JOINT WMO TECHNICAL PROGRESS REPORT ON THE GLOBAL DATA PROCESSING AND FORECASTING SYSTEM AND NUMERICAL WEATHER PREDICTION RESEARCH ACTIVITIES FOR 2017

Croatian Meteorological and Hydrological Service (DHMZ)

1. Summary of highlights

Several new models for air quality modeling were set up and used at DHMZ. Nowcasting system was installed on new server and new observations were added.

2. Equipment in use at the Centre

The computer used for the forecasting system is an SGI UV 2000 (***Figure 1*** and ***Table 1***). The storage is Quantum Scalar i500 and the visualization is based on Grads, Magics, Metview, Python and R.

Table 1. *Computers used operationally.*

Computer	Memory	Storage
Model forecast: SGI UV 2000	1075 GB	7.1 TB
Storage: Quantum Scalar i500	8 GB	59TB disc + tapes
Visualization: Linux server	125 GB	3.5 TB

Model forecast:

- SGI UV 2000
- 48 Intel Xeon E5 6core 2,9GHz 15MB cache CPUs with total 288 cores
- 1075 GB RAM
- working disks 7.1TB
- Intel compilers version 13.1.0 20130121
- PBSPro, SGI management software, Fibre Channel, Gigabit Ethernet

Storage:

- Quantum Scalar i500
- OS SUSE Linux Enterprise Server 10 for IPF with SGI Package
- 59Tb online data + tapes

Main users: NWP, Air-quality modeling & Climate modeling

Figure 1. Operational computer system at DHMZ.

3. Data and Products from GTS in use

- SYNOP
- TEMP
- AMDAR
- SHIP
- FAX
- GRIB
- BUFR

4. Forecasting system

4.1 System run schedule and forecast ranges

Two operational configurations of Limited Area Model with 4km (ALADIN-HR4) and 8km horizontal grid spacing (ALADIN-HR8) are run four times per day (00, 06, 12, 18 UTC) for 72 hours ahead using lateral boundary conditions (LBC) from ECMWF global model in so-called *lagged mode*. Lagged mode is used because of time constrains for ALADIN forecast and times of availability of ECMWF forecast. In lagged mode there is 6 hours shift between initialization time of global model and local ALADIN model e.g. for ALADIN-HR4 forecast initialized at 00 UTC, ECMWF forecast initialized at 18 UTC is used for LBC. ALADIN-HR4/HR8 forecast are dynamically adapted to the 2 km resolution topography in a procedure (DADA) designed to improve high resolution wind forecast, especially in case of severe wind events. The procedure is performed for each output file of the ALADIN-HR4/HR8 forecast with 1-hourly frequency. The high-resolution ALADIN full model forecast with 2 km horizontal grid spacing (ALADIN-HR2) is run only once per day. The initial file is interpolated 6 hour forecast of the ALADIN-HR8 run that started at 00 UTC. The forecast range is 24 hours and covers the observing period of the rain gauges. Forecast ranges and product availability times are shown in ***Table 2***.

Table 2. *The main features of the operational model runs.*

Suite	Initialization time [UTC]	Initial conditions	LBC	Start time	End time	Products availability
ALADIN-8	00 / 06 / 12 / 18	Assimilation	ECMWF	+03:15h	+03:45h	+03:50h
ALADIN-4	00 / 06 / 12 / 18	Assimilation	ECMWF	+02:00h	+03:00h	+03:05h
ALADIN-2	06	ALARO-8 (00UTC)	ALARO-8 (00UTC)	03:25 UTC	04:10 UTC	04:15 UTC

4.2 Medium range forecasting system (4-10 days)

There are three global model products available. The IFS operational forecast output is available from ECMWF, GME from DWD and the ARPEGE model output is available from Meteo-France.

4.3 Short-range forecasting system (0-72 hrs)

The operational ALADIN-HR4/HR8 is run four times per day, initialized from local data assimilation cycle, with 6h cycle frequency for ALADIN-HR8 and 3h cycle frequency for ALADIN-HR4. The operational forecast is run 72 hours ahead on a Lambert-projection domain with 4(8)km horizontal resolution with 73(37) hybrid sigma-pressure levels in the vertical. ALADIN-HR4 configuration became operational from the end of November 2016. From 1 January 2014 LBC from ECMWF are used operationally (Tudor et al 2015a).

The model forecast fields from ALADIN-HR8 run are subsequently going through a dynamical adaptation procedure (Ivatek-Šahdan and Tudor, 2004) that produces a 2-km resolution forecast of 10 m wind speed and gusts. The dynamical adaptation method of Žagar and Rakovec (1999) has been adapted for the purpose of operational forecast of the 10 m wind. The method provides successful operational forecast of the 10 m wind (Ivatek-Šahdan and Tudor, 2004) and is used extensively in research impact studies (Bajić et al., 2007) as well as case studies of severe wind (Tudor and Ivatek-Šahdan, 2002).

The model fields are first interpolated from the low resolution (8 km in this case) to a higher resolution (2 km) grid, but at a considerably lower number of model levels – at 15 out of 37 vertical levels. The number of vertical levels is reduced to minimize computational cost. The levels close to the ground are of similar density, and the higher levels are mostly omitted. Then a hydrostatic version of the ALADIN model is run for 30 time steps with a 60-second time step. The same large-scale model data are used as initial and boundary conditions, therefore the fields at lateral boundaries do not change during the adaptation procedure. Turbulence is the only parameterization scheme used. Contributions from the moist and radiation processes are not computed in order to accelerate the model integration. .

Also 2-km resolution 24-hour forecast is performed once per day, with non-hydrostatic (NH) dynamics in the ALADIN model and the full parameterization set, including the convection scheme (ALADIN-HR2). This forecast is performed once per day, following the 00 UTC operational 8-km forecast. It uses the 6-hour forecast from the 8-km operational run as an initial file and is run with the Scale-Selective Digital Filter Initialization (SSDFI). This high-resolution forecast is then integrated for 24 hours, until 6 UTC on the next day. This procedure covers the 24-hour period allowing the collection of precipitation data from rain gauges.

4.3.1 Data assimilation, objective analysis and initialization

4.3.1.2. In operation

The assimilation system is for ALADIN-HR8 is operational from November 2011 and for ALADIN-HR4 full data assimilation system (surface and upper air assimilation) became operational from the end of November 2016. The assimilation system consists of two parts: surface assimilation, which is used to initialize the state of the modeled land surface variables, and the upper-air assimilation (***Figure 2***). Surface assimilation is made by the optimal interpolation (OI) technique, while the upper-air assimilation is conducted using the 3D Variational technique (3DVAR). Surface assimilation uses 2 m temperature and relative humidity observations. For upper-air assimilation the following observations are used: SYNOP, TEMP, AIREP, wind-profiler and measurements from polar and geostationary satellites (***Table 3***). Observational data is available through local exchange facility (OPLACE - Observation Pre-processing for LACE) installed and maintained in the Hungarian Meteorological Service in Budapest. In addition, the data-assimilation suite uses the data from the network of automatic stations of Croatia. More details about assimilation setup can be found in Stanešić (2011).

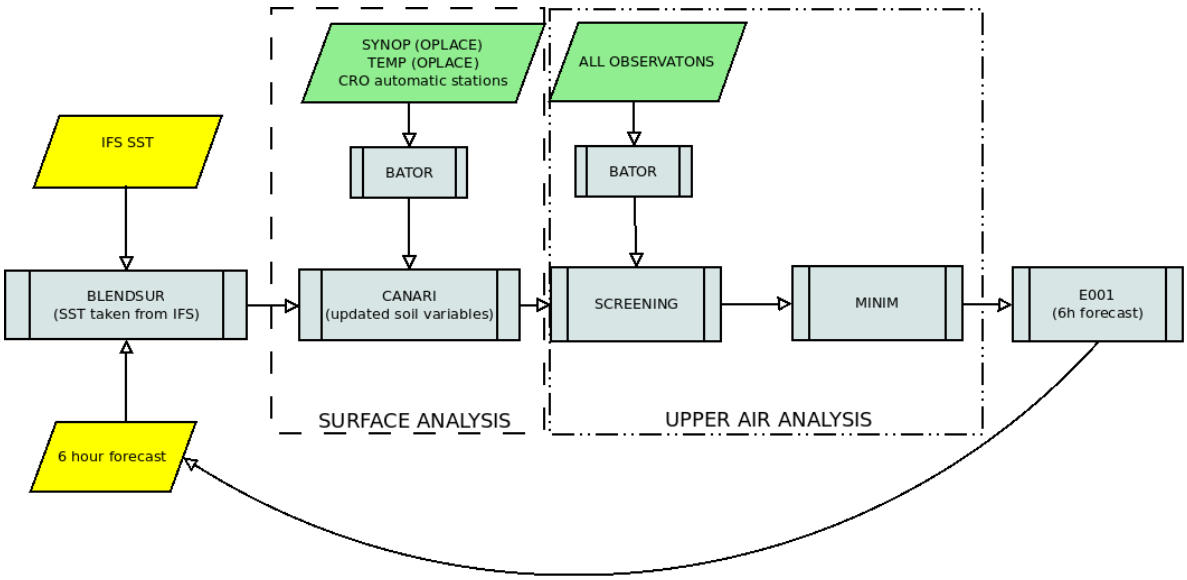

Figure 2. *Scheme of assimilation cycle at DHMZ.*

The forecast error for ALADIN-HR4 is approximated by a set of forecast differences valid at the same verification time, but at different forecast ranges, the so-called standard NMC method of background error-matrix (B matrix) calculation. The model runs for B matrix calculation were initialized with a 24-hour time difference using forecast ranges +36h and +12h forecasts for calculations. Calculation of sensitivities varied initialization time (00, 06, 12 and 18 UTC) and month (January, May and August 2014). In addition, average matrices over all forecast ranges and over all months are calculated. The analysis of results suggested that the optimal B matrix for operational use is averaged over January, May and August 2014, thus calculated with 90 forecast differences. In this manner, four different B matrices are calculated and used operationally for 00 UTC, 06 UTC, 12 UTC and 18 UTC. The B matrix is isotropic in the horizontal and follows a multivariate formulation of vorticity, divergence, temperature and surface pressure and specific humidity as the control variables. The operational B matrix is tuned based on the method proposed by Desroziers et al (2005).

For ALADIN-HR4 analysis cycle is executed every three hours using a long cut-off observational data and LBCs. Similar procedure is done for the production, only difference is that a short cut-off data and LBCs are used and at the end 72-hour forecast is performed. At the beginning of 72-hour forecast, digital filter initialization (DFI; Lynch, 1997) is applied while DFI is not used in assimilaton cycle.

For the ALADIN-HR2 a SSDFI is used to initialize the fields, since the usual DFI removes some meteorological high resolution features from the initial model fields (Termonia, 2008).

Table 3. *Observations used in the ALADIN-HR4 assimilation system.*

Observation system	Assimilated fields
SYNOP	T2m,RH2m,p
AMDAR/MODE-S	U,V,T
TEMP	U,V,T,Q, Φ
GEOWIND	U,V
MSG SEVIRI	radiance

4.3.2 Model

4.3.2.1 In operation

The model system for the short range weather forecast used at Meteorological and Hydrological Service (DHMZ) is ALADIN. The same integration domain for 8-km resolution run (ALADIN-HR8) and 4-km resolution run (ALADIN-HR4) is used and it is shown in ***Figure 3*** and the domain for the 2-km resolution run (ALADIN-HR2) is shown in ***Figure 4***. The main characteristics of the operational forecast model (see Tudor et al 2015a) are listed in ***Table 4***.

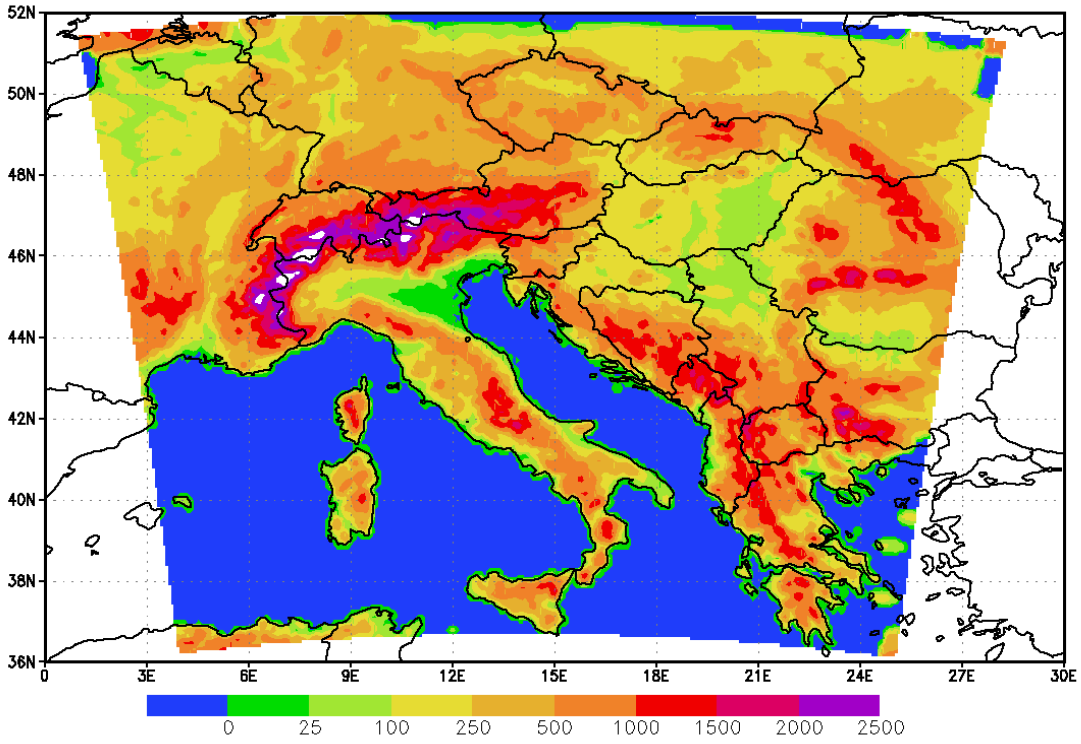

Figure 3. *Domain and model topography (shaded, in meters) of ALADIN-HR8 km resolution run, 11 rows on the northern edge and 11 columns on the eastern edge are the extension zone.*

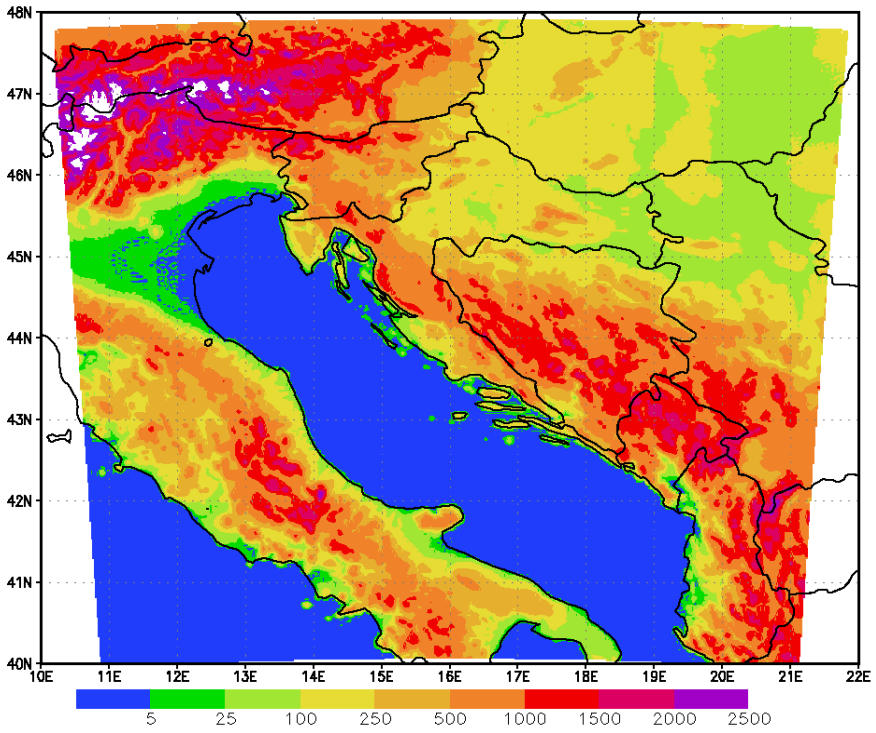

Figure 4. *Domain and model topography (shaded, in meters) of ALADIN-Croatia 2km resolution non-hydrostatic run and high-resolution dynamical adaptation.*

Horizontal diffusion in NWP models is employed to suppress the accumulation of energy at the shortest wavelengths. In ALADIN system this used to be achieved by a common 4^{th} order numerical diffusion at the end of each time step. The semi-Lagrangian horizontal diffusion (SLHD) is computed by combining two semi-Lagrangian interpolators of different diffusivity with the flow deformation as a weighting factor. This procedure yields an improved horizontal diffusion scheme that is based on the physical properties of the flow (Vana et al., 2008). The SLHD is used in parallel model versions since December 2006 and it is fully operational since February 2008.

The ALARO0 physics parameterization package includes prognostic schemes for turbulence, microphysics and convection. The turbulent exchange coefficients are computed using prognostic values of turbulent kinetic energy (TKE) according to Geleyn et al. (2006). Contribution of shallow convection is computed using the moist turbulence scheme from Geleyn 1988.

The parameterization scheme for land surface, Interaction Soil Biosphere Atmosphere (ISBA; Noilhan and Planton, 1989), is used in operational forecast as well as in the surface data assimilation (Giard and Bazile, 2000).

Cloud microphysics describes the processes of condensation, evaporation, freezing and melting as well as the processes that transform the cloud water droplets and ice crystals into rain and snow. A simple microphysics scheme is used with prognostic cloud water and ice, rain and snow (Catry et al., 2007) and a statistical approach for sedimentation of precipitation (Geleyn et al., 2008).

Table 4. *Model characteristics in different model runs.*

	ALADIN-HR8	ALADIN-HR4	2km HRDA	ALADIN-HR2
Horizontal resolution	8 km	4 km	2 km	2 km
Spectral truncation	(quadratic) 79x71	(quadratic) 159x143	(quadratic) 149x149	(quadratic) 149x149
Number of levels	37	73	15	37
Number of grid points	240x216	480x432	450x450	450x450
Time step (sec)	327.273	180	60	60
Forecast range (hrs)	72	72	72	24
Initialization	OI + 3Dvar	OI	No	SSDFI
Coupling model	IFS	IFS	ALADIN 8km	ALADIN 8km
Coupling freq. (hrs)	3 (Davies relaxation)	3 (Davies relaxation)	constant LBCs, (Davies relax.)	1 (Davies relaxation)
Output frequency (hrs)	1 and 3	1 and 3	1 and 3	1
Dynamics	Hydrostatic, 2 time level, semi implicit, semi lagrangian	Hydrostatic, 2 time level, semi implicit, semi lagrangian	Hydrostatic, 2 time level, semi implicit, semi lagrangian	non-hydrostatic, 2 time level, semi implicit, semi lagrangian
Orography	Mean	Mean	mean	mean
Grid (gp and spec)	A, quadratic	A, quadratic	A, quadratic	A, quadratic
Physics	ALARO0	ALARO0	Turbulence only	ALARO0
Horizontal diffusion	SLHD	SLHD	SLHD	SLHD

The convective processes redistribute momentum, heat and moisture in the vertical. Within ALARO0 physics package, there is modular multi-scale micro-physics and transport (3MT) scheme for precipitation and clouds (Gerard and Geleyn, 2005; Gerard, 2007; Gerard et al., 2009). The scheme uses prognostic variables for up-draft and down-draft vertical velocities and mesh fractions, entrainment and convective clouds. The 3MT scheme is operational since January 2015.

The processes of condensation, evaporation, freezing, melting, aggregation and growth of cloud water and ice into rain and snow are described by the micro-physics. Prognostic scheme for the cloud water and ice, rain and snow and a statistical approach for sedimentation of precipitation (Geleyn et al., 2008) is derived upon the old diagnostic scheme based on the Kessler (1969) type scheme with modifications (Geleyn et. al. 1994). The scheme is re-tuned in order to avoid fibrillations that occur due to a combination of melting and sublimation parameters (Tudor, 2013).

The transfer, scattering, absorption and reflection of the short-wave solar radiation and long-wave thermal radiation of the Earth's surface and clouds are parameterized in radiation scheme (Geleyn and Hollingsworth, 1979, Ritter and Geleyn, 1982). The scheme uses only one spectral band for

long-wave and one for short-wave radiation. The net exchange rate has been introduced in the scheme (Geleyn et. al. 2005a, 2005b) and recently switched on in the operational forecast set-up. This radiation scheme is computationally cheap, so the computations are done each model time-step, avoiding possible numerical instability (Pauluis and Emmanuel, 2004).

The vertical transfer of heat, momentum and moisture due to impact of the unresolved motion and surface roughness are described by turbulence parameterization that uses prognostic turbulent kinetic energy (TKE) that is advected, diffused (Geleyn et al., 2006) combined with modified Louis (1979) dependency on stability (Redelsperger et al., 2001). The contribution of the shallow convection to the evolution of model variables is computed in the turbulence scheme (Geleyn, 1987).

Wind, temperature and humidity are interpolated from the model levels to the standard meteorological measurement heights (10 and 2 meters above surface) using a parameterized profile (Geleyn, 1988).

Wave model forecast

In order to provide forecast of height and direction of wind waves, model has been ported and set up to perform daily runs. The Wind Wave Model (WWM) is an unstructured grid spectral wave model. It incorporates most existing source term formulation for wind input and dissipation. It uses residual distribution schemes for the horizontal advection. It integrates the wave action equation (WAE) by using the operator splitting method in explicit or implicit mode.

The WWM model was set up to use the wind output from the ALADIN model. Model runs for 36 hours starting at 0000 UTC, limited by the available wave model data. Runtime is 20 minutes on 66 processors. Time step is 5 minutes for the implicit scheme. Figures are automatically created both for the whole Adriatic and for the Istrian region. The model is run with boundary data at the Otranto strait obtained from the global WAM model run at ECMWF. Model data is interpolated in time, space and spectrum to the boundary. The spectral resolution uses 36 direction and 36 frequencies with the minimal frequency at 0.045 Hz and maximum at 1.26 Hz. This is distinct from the resolution used at ECMWF with minimum frequency 0.036 Hz and maximum at 0.98 Hz but explained by the need to cover the short waves in the enclosed Adriatic Sea. The exponential increment in frequency is set to the standard 1.1 value.

The grid that we used for the modelization is a unstructured grid with 84743 nodes, 135069 elements, and a resolution that varies between 10m and 4km. 435 islands are resolved by this grid which is a relatively large number.

The model is integrated using an implicit scheme that this writer authored. The scheme integrates the whole Wave Action Equation by an iterative scheme. It is based on a Jacobi scheme and uses block Gauss Seidel on processors in order to speed up the convergence. Further analysis showed that there are ways to increase the speed by not treating regions where convergence has been achieved and that will not be further modified. However, since the speed was sufficient with the existing scheme, I choose not to implement it right away.

The comparison of model forecast is done with the Altimeter. The data used for the comparison is from IFREMER which collects the GDR data set and updates them every 6 months. We found the comparison with OPR altimeter data to be unreliable due to numerous artifact and lack of postprocessing.

Comparison with JSAON 2 satellite of wind speed yields the following scatter plot diagram.

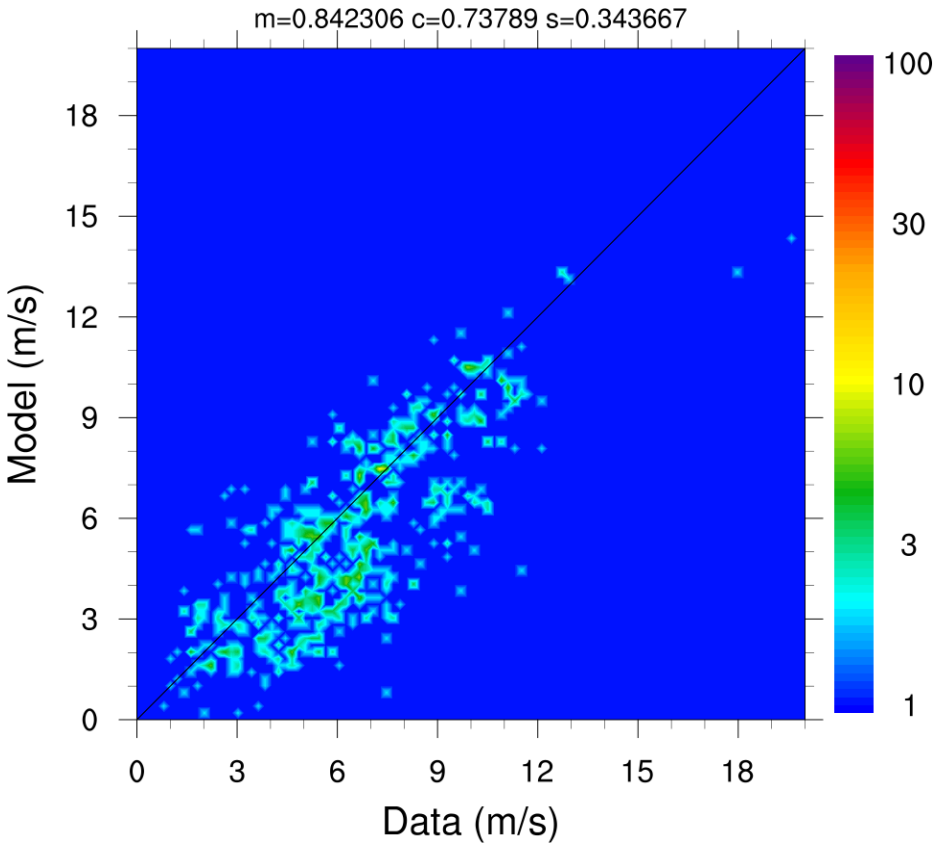

While the comparison with significant wave height of the model shows the following diagram.

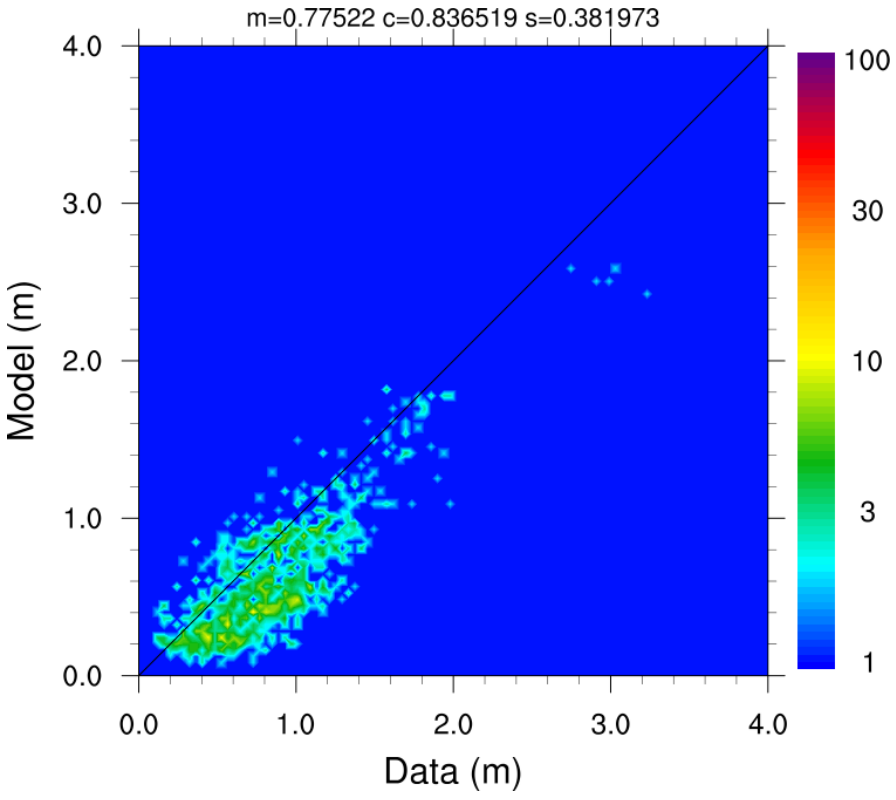

This shows that there is still large room for improvements of the model since the scatter index s should be smaller for the waves than for the wind.

4.3.2.2 Research performed in this field

B matrix calculation

New background error covariance matrix for ALADIN-HR4 model was calculated using ensemble method (ENSLBC). The ensemble B matrix was compared with NMC B matrix (NMC) by looking at diagnostic plots and by assessing influence on analysis and forecast. Additionally, influence of LBC perturbation on characteristics of B matrix was estimated. Results showed that LBC perturbations influence all control variables with the smallest influence found for specific humidity. Diagnostic comparison showed that ensemble technique shifts correlations towards small scales while LBC perturbations give rise to long scales. Influence on analysis showed smaller spatial correlation for ensemble B matrix compared to NMC, with again most pronounced differences for specific humidity (Figure 5).

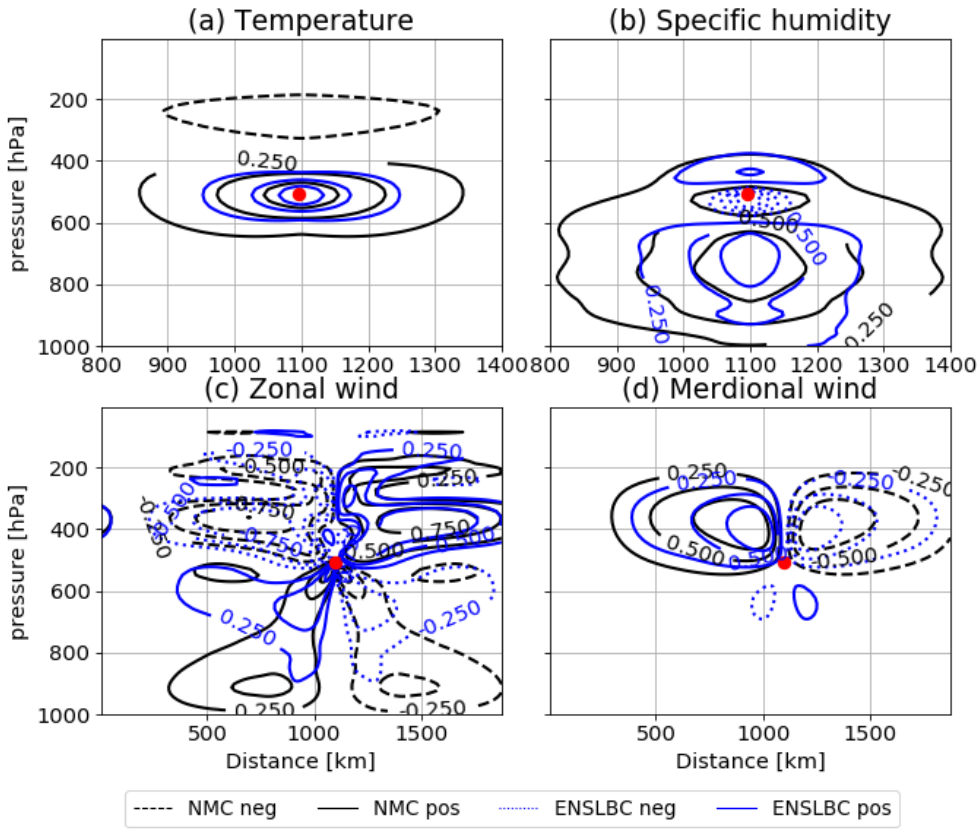

Figure 5 Vertical cross section of analysis increment due to single radiosonde temperature observation having innovation of 1K at ~500hP normalized by its maximum value and plotted with contours having levels from -1 to 1 with 0.25 increment for (a) temperature, (b) specific humidity, (c) zonal wind component, (d) meridional wind component. Zero contour line was omitted for maintaining clearness of plot. Experiment where ENSLBC B matrix was used was denoted with blue full lines for positive values and blue dotted lines for negative values while experiment where NMC B matrix was used was denoted with black full

lines for positive values and black dashed lines for negative values. Location of observation was marked with red dot.

Clear benefit of using ENSLBC B matrix on internal model balances in the analysis was demonstrated by calculating and plotting of temporal evolution of surface pressure tendency (Figure 6).

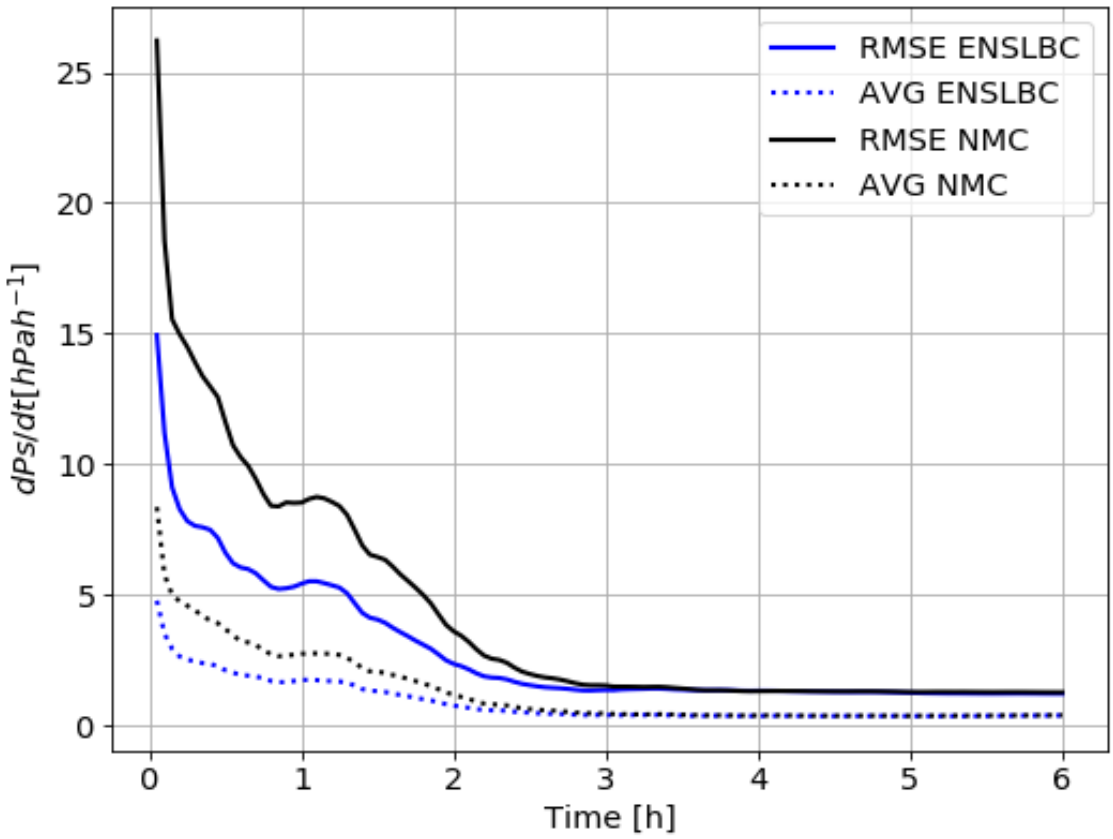

Figure 6 Temporal evolution of the surface pressure tendency mean (dashed line) and root-mean-square (full line) averaged over the model domain and over 11 forecasts as function of the forecast range for ENSLBC (blue) and NMC experiment (black).

Verification of forecast gave modest improvement for experiment with ensemble B matrix.

Infulence of surface roughness on downslope windstorms and mountain waves

Here we analyse the effect of surface friction in the framework of the ALADIN System, particularly the version used for operational forecast at 2 km horizontal grid spacing with ALARO physics package and non-hydrostatic dynamics. The problem is analysed using the real terrain and real meteorological conditions. Surface friction is controlled via the surface roughness field. In order to assess the relative importance of the surface friction to the turbulence scheme, experiments with two different turbulence schemes were performed: I) a pTKE scheme and II) more advanced TOUCANS, which includes additional prognostic equation for total turbulence energy, as well as the anisotropy effects among other.

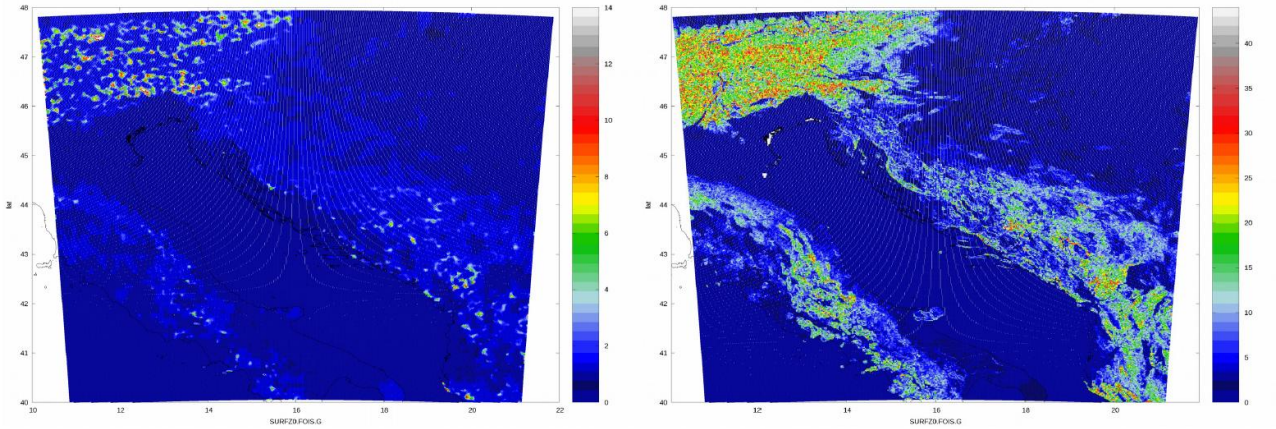

Figure 7 The surface roughness used in the model: old (left) and new (right).

The impact of modified roughness length was tested by running 31 consecutive forecasts at 2 km horizontal grid spacing (Tudor and Ivatek-Šahdan, 2010) starting from 00 UTC 1st of March 2016. The forecast using low roughness length (from the old database) occasionally produced excessive wind speed for location Knin in a valley downstream of a mountain during bura episodes. Simultaneously, wind speed was underpredicted for another location (Lokvine) which is in the lee of a mountain about 50 km westward from Knin. The experiments have shown that this windstorm develops due to too smooth mountains (which is unrealistic). The introduction of roughness length from the new database made the terrain rougher in general. When using this more realistic and larger surface roughness field, the windstorm did not develop over Knin, but it did over Lokvine, which better corresponds to the measurements .

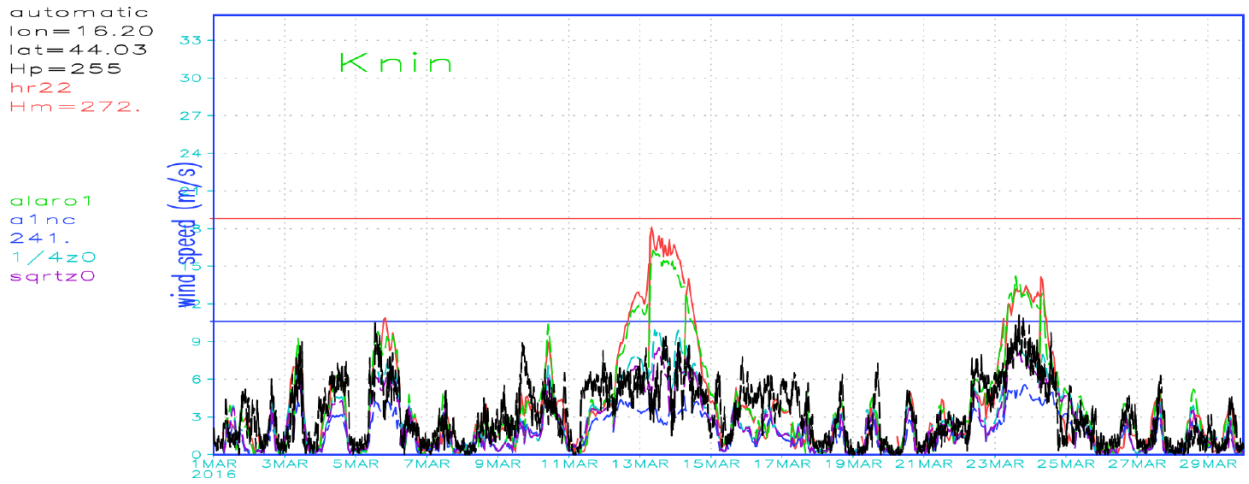

Figure 8 Measured (black(and forecast 10m wind in Knin for March 2016: using old z0 and pTKE (red), old z0 and TOUCANS (green), new z0 and TOUCANS (blue), 0.25 new z0 (light blue) and sqrt(new z0) (violet).

Surface roughness is recomputed using new terrain database. The field used in the operational forecast computed from a low resolution database had small values making Dinaric Alps very smooth. It impacts the wind field forecast as well as the small scale dynamics features that develop over mountains and in valleys between. More realistic surface roughness allowed for model dynamics to develop local features at appropriate place and time and produce more accurate 10-m wind forecast. The effect is the same for the old TKE scheme and if the new TOUCANS turbulence scheme (Bašták Ďurán et. al. 2014).

Other models

The WRF models is being run in large-eddy simulation (LES) research mode for specific research purposes at the research department, such as case studies of extreme winds in complex terrain, convection and heavy precipitation, internal gravity waves, meteotsunamis, near-surface wind shear, and other. Various setups are currently tested, including varying grid spacing, PBL parametrizations, convection schemes, microphysics schemes, type of nesting etc. Current tests focused on high-resolution modelling of wind speed variability in very complex terrain of the eastern Adriatic coast and comparing of results we achieved for the western US. The grid spacing used in this study reached grid spacing of 37 m and assessed the ability of the model to simulate wind variability on the order of seconds. The simulations used ECWMF operational analysis for initial and lateral boundary conditions. Further tests are planned using the WRF model with LES closure instead of PBL parametrization, as well as testing several subfilter parametrizations.

Table 5(left) Comparison of mesoscale and LES simulation parameters for numerical simulation of mid-Adriatic Bora test case on 28 Apr 2010 at location Pometeno brdo, hinterland of Split, Croatia.

	Mesoscale (d04)	LES (d06)
dx	333 m	37 m
dt	1,48s	0,164s
PBL	MYNN2.5L TKE	-
diffusion	Coordinate surfaces (vertical diffusion by PBL)	3D physical space x,y,z
Eddy coefficient	2D horizontal Smagorinsky first-order closure	1.5 order TKE closure
Output archived	1 min	5 sec

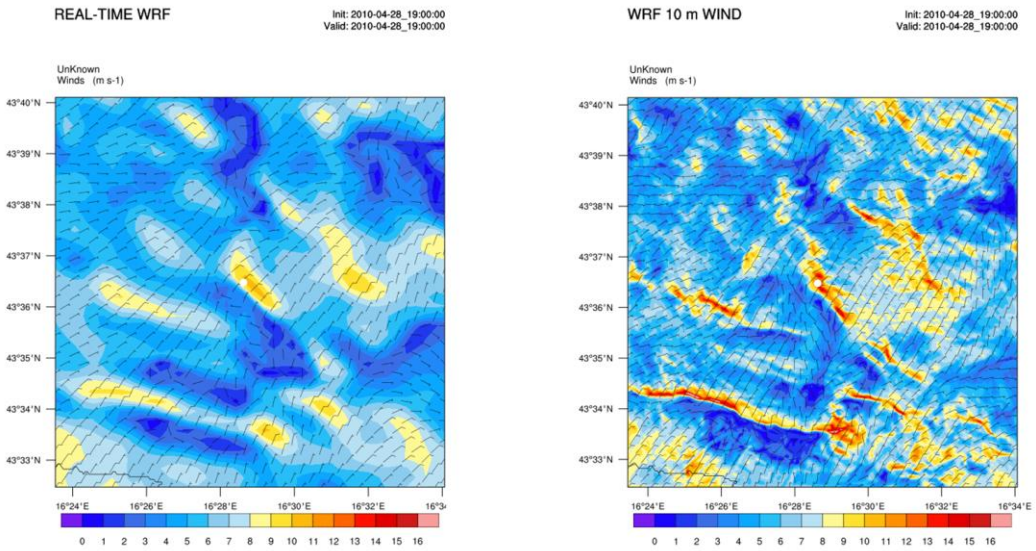

Figure 9 Comparison of wind field in section of domain of 14 km x 14 km using mesoscale simulations (dx=333 m) and LES simulations (dx=37 m) for mid-Adriatic Bora test case on 28 Apr 2010 at location Pometeno brdo, hinterland of Split, Croatia

4.3.3 Operationally available NWP products

Output variables of the 8km resolution run (3 hourly outputs):

- 3D: u, v, omega (Pa/s), geopotential, vorticity, divergence, absolute and potential vorticity, temperature, potential and equipotential temperature and relative moisture on pressure levels (1000, 975, 950, 925, 900, 850, 800, 700, 600, 500, 300, 250 hPa);
- 2D: u, v 10m above ground, temperature and relative humidity 2m above ground, low, medium, high and convective cloudiness, stratiform and convective rain and snow, mean sea level pressure, wind gusts u and v components, CAPE, moisture convergence, PBL height, and the Showalter, Sweat, k-index and totals-totals (in)stability indices,
- 2D: pre-defined vertical cross sections of wind, temperature, humidity, potential temperature, vertical velocity, TKE and snow.

Output variables of the ALADIN-HR4/HR8 model (1 hourly output):

- 3D: model output fields used for initial and LBCs of the 2km resolution model runs
- values at approximately 300 pre-defined model points of mean sea level pressure, cloudiness (low, medium, high, convective), precipitation (rain and snow), 2m temperature and humidity, 10m wind speed, direction and gusts used for meteograms,
- upper level values of potential temperature, humidity, wind speed and direction used for the high-resolution isentropic analysis (HRID).

Output variables of the 2km resolution dynamical adaptation of the wind field:

- 10m wind speed, direction and gusts figures are produced 3 hourly, data are hourly,
- Wind speed and direction at 80m for locations of wind farms (Figure 10)
- pre-defined vertical cross-sections of potential temperature wind speed and direction.

Output variables of the ALADIN-HR2 non-hydrostatic forecast (hourly outputs):

- 3D: u, v, omega (Pa/s), geopotential, potential vorticity, potential temperature and relative humidity on pressure levels (1000, 975, 950, 925, 900, 850, 800, 700, 600, 500, 300, 250 hPa);
- 2D: u, v 10m above ground, temperature and relative humidity 2m above ground, low, medium, high and convective cloudiness, stratiform and convective rain and snow, mean sea level pressure, wind gusts u and v components, CAPE, moisture convergence PBL height, and the Showalter, Sweat, k-index and totals-totals (in)stability indices.

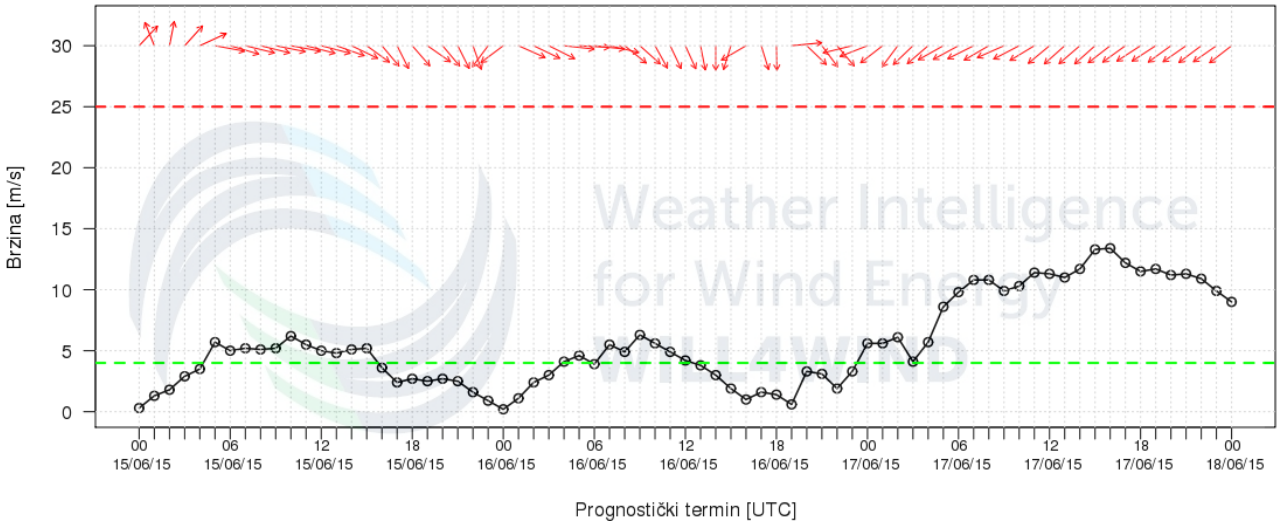

Figure 10. *Wind speed and direction at 80m at location of one wind farm. On x axis forecast hour in UTC is given, while on y axis wind speed in m/s is shown. Wind direction is indicated by red arrows.*

4.3.4 Operational techniques for application of NWP products (MOS, PPM, KF, Expert Systems etc.)

4.3.4.1 In operation

From the end of November 2016 the Analog-based method is used to provide forecast of wind speed for 16 locations. The Analog-based method is a state-of-the-art technique used for point-based forecasting. It is based on finding the most similar past numerical weather predictions (analogs) over several variables (predictors), and then forming an analog ensemble (AnEn) out of the corresponding observations. The operational Analog-based method uses four 2 km HRDA operational output products as predictor variables: wind speed and direction, vorticity and divergence. The Analog-based 3-hourly wind speed output (up to +72 hours) is visualized by boxplot figures (**Figure 11**a), representing 15-members ensemble. To produce deterministic Analog-based wind speed forecast, AnEn members are averaged for every lead time. Besides improving a deterministic forecasting system, there is also need for reliably expressing its uncertainty. The Analog-based method can be used to produce probabilistic forecasts, where the forecast probability density function may be estimated from the members of the AnEn. One example of such forecast is shown on **Figure 11b**. The application of Analog-based method has

been thoroughly tested and the results are accepted to be published at Journal of Applied Meteorology and Climatology (Odak Plenkovic et al., 2018). Currently, the new algorithms are being developed to expand the number of locations and the forecast variables.

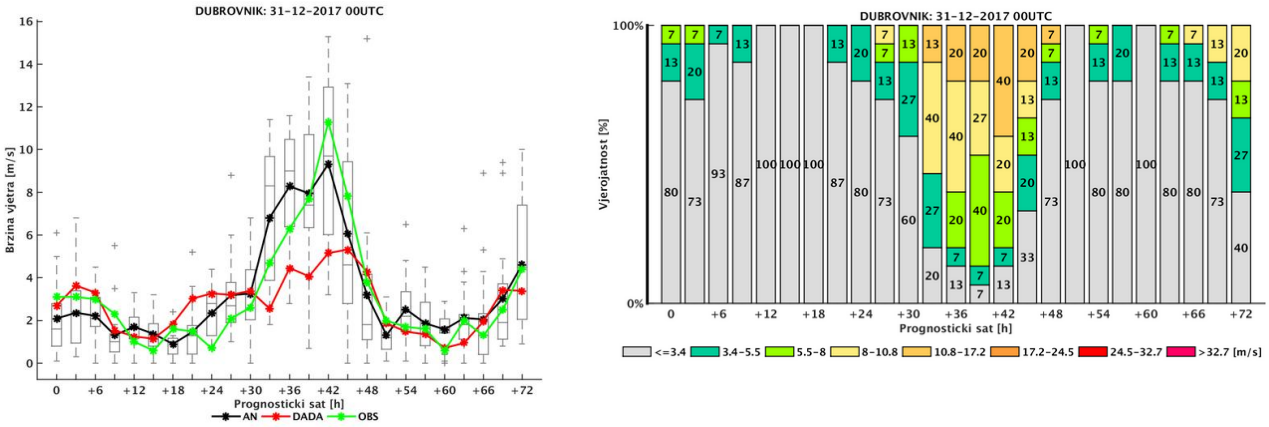

Figure 11. *Wind forecast product from Analog-based method with deterministic (left) and probabilistic (right) forecast. On left figure AnEn forcast is black, observations are green and ALADIN model forecast (2 km HRDA) is red.*

4.3.4.2 Research performed in this field

4.3.5 Ensemble Prediction System

4.3.5.1 In operation

The operational LAMEPS system is maintained by ZAMG-Austria and developed by RC-LACE.

4.3.5.2 Research performed in this field

Team members were involved in the development of the ALADIN_LAEF system in ZAMG.

4.3.5.3 Operationally available EPS Products

ECMWF EPS and ALADIN-LAEF products are available to forecasters.

Outputs of other operational ALADIN models run in other LACE countries together form an ensemble of forecasts since all meteorological services run different model versions and data assimilation/initialization set-ups.

4.4 Nowcasting and Very Short-range Forecasting Systems (0-6 hrs)

4.4.1 Nowcasting system

4.4.1.1 In operation

In the operational forecast service nowcasting is primarily based on METEOSAT satellite data, received through EUMETCast service, radar data from two Doppler radars located in the continental part (Bilogora and Osijek) and lightning data from LINET lightning detection network and ATD NOS system (Met Office).

Satellite data

- Meteosat Second Generation single channel data

- RGB images and image differences: all standard RGB images are available in 15 or 5 min (Rapid Scan Service) intervals, DAWBEE User Station used for processing and visualization of satellite data

Satellite-based Nowcast products

- Locally developed post-processing products based on satellite data

- EUMETSAT MPEF (Meteorological Products Extraction Facility) products received through EUMETCast service

- NWC SAF (Satellite Application Facility on support to Nowcasting/ and Very Short-Range Forecasting) products calculated by locally installed NWC SAF software using METEOSAT data ECMWF NWP and lightning data.

Products are received or calculated with each satellite scan (mostly in 15 min cycle) and displayed in the forecast intranet system.

INCA

The high-resolution analysis and nowcasting system developed at ZAMG, Austria has been implemented at DHMZ. INCA (Integrated Nowcasting through Comprehensive Analysis) combines forecast fields of the numerical weather prediction model ALADIN and high-resolution topographic data with measurements from surface station data and remote sensing data (radar, satellite). The system operates at a 1-km horizontal resolution and with vertical resolution of 100-200 m. In the current implementation at DHMZ, the INCA system provides analysis of 2-meter temperature, humidity and 10-meter wind on an hourly basis. Also two-dimensional maps of some derived

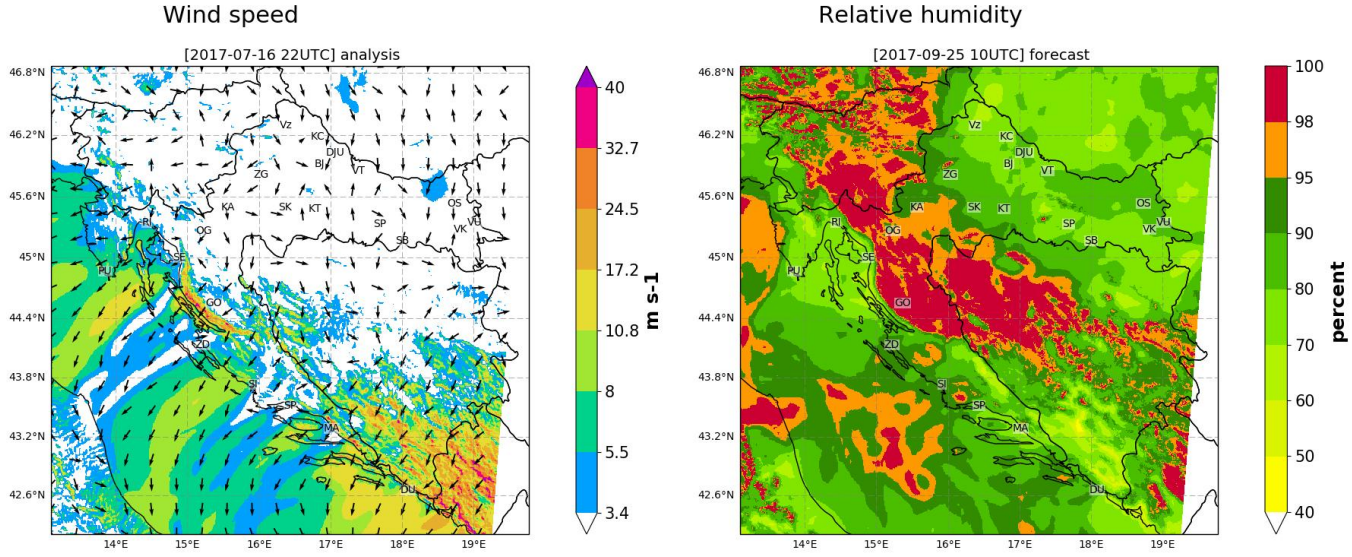

quantities (e.g. CAPE, CIN, LFC, wind chill …) are available. INCA has been installed on a new server and new observations have been added for analysis mode. The nowcasting part of INCA has been implemented with weather prediction model ALADIN 4km as its background. Extensive technical manual for its implementation and use has been made as well as new visual interface. The precipitation module has not yet been implemented, as significant work is still needed for the adjustment of these data.

Figure ***12.*** *INCA wind speed analysis field (left) and INCA forecast relative humidity field (right)*

4.4.1.2 Research performed in this field

4.4.2 Models for Very Short-range Forecasting Systems

4.4.2.1 In operation

4.4.2.2 Research performed in this field

4.5 Specialized numerical predictions

4.5.2 Specific models

4.5.2.1 In operational

4.5.2.2 Research performed in this field

4.5.2.2.1. Air quality modelling

EMEP model. Open-source version of the EMEP rv4.10 (European Monitoring and Evaluation Programme) is installed and running at MHSC (Figure 13). Unified EMEP models are the chemical transport models used and developed at the Norwegian Meteorological Institute (Simpson et al, 2003). It simulates atmospheric transport and deposition of acidifying and eutrophying compounds, as well as photo-oxidants and particulate matter over Europe. Meteorological input data used for the model are based on Integrated Forecast System (IFS) data, a global operational forecasting model from the European Centre for Medium-Range Weather Forecasts (ECMWF). The IFS forecasts have been run by MSC-W as independent experiments on the HPCs at ECMWF with special requests on some output parameters. The meteorological fields are retrieved on a 0.2x0.2 rotated spherical grid and interpolated to 50x50 km^2 polar-stereographic grid projection. Vertically, the fields on 60 eta levels from the IFS model are interpolated onto the 20 EMEP sigma levels.

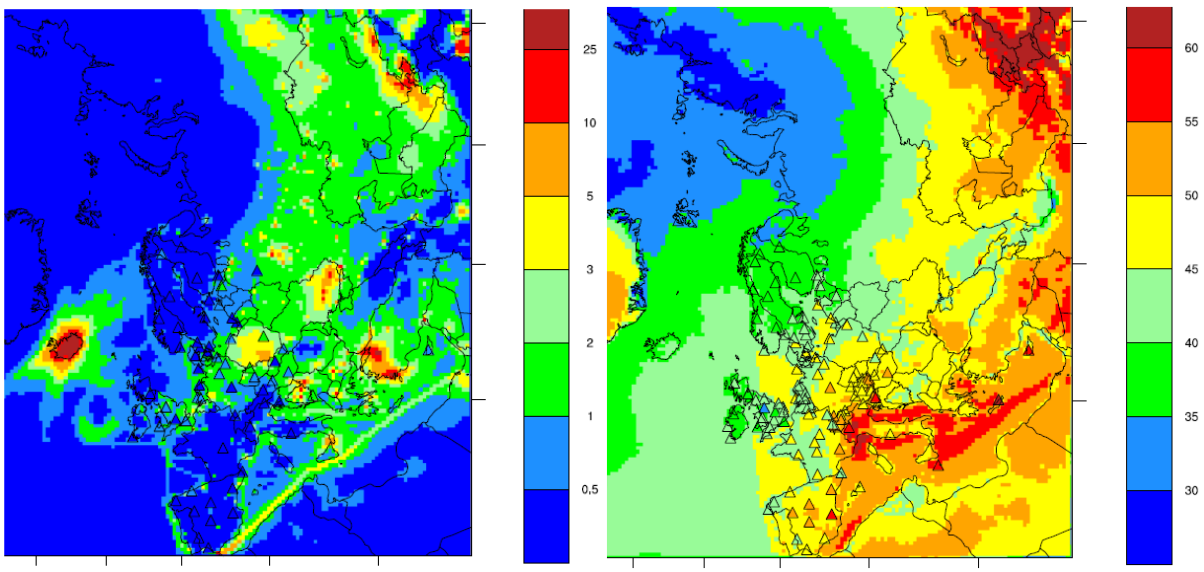

Figure 13 Results of the EMEP rv4.10 model coupled with ECMWF for NO2 (µg/m3, left) and ozone (ppb, right).

LOTOS-EUROS model (LOng **T**erm **O**zone **S**imulation - **EUR**opean **O**perational **S**mog model). New open-source version of the model has been installed and tested at MHSC during 2016. Model

is developed by TNO Institute of Environmental Sciences, RIVM National Institute for Public Health and the Environment, KNMI Royal Netherlands Meteorological Institute and PBL Netherlands Environmental Assessment Agency and promoted as an open-source model in 2016.

The LOTOS-EUROS-model is an Eulerian grid model covering Europe (Iceland excluded with horizontal boundaries at 10W and 60E and at 35N and 70N. In horizontal direction the model domain in its standard version is divided into 140x140 grid cells with a size of 0.5 deg lon.x 0.25 deg lat. (~25-30x25-30 km2). There is a possibility to zoom in by a factor 2 or 4 to a resolution of ~6-7x6-7km2. In the standard model version the lowest 3.5 km of the atmosphere are represented by three terrain following prognostic layers for which the continuity equation is solved and an additional (diagnostic) surface layer of 25 meter. The lowest of the three prognostic layers is the boundary layer, the two other layers are reservoir layers. The two reservoir layers are of equal depth but vary in time. The purpose of these layers is to keep track of pollutants emitted above the boundary layer under stable conditions. They also serve as reservoir for aged pollutants entrained and detrained during multiday episodes. Exchange of pollutants with the free troposphere takes place through the top layer. For each of the three prognostic layers and for each long-lived (transportable) species a time dependent continuity equation is solved.

The LOTOS-EUROS system in its standard version is driven by 3-hourly meteorological data. These include 3D fields for wind direction, wind speed, temperature, humidity and density, substantiated by 2D gridded fields of mixing layer height, precipitation rates, cloud cover and several boundary layer and surface variables. Meteorological driver for the model are: operational IFS forecast for the day before, ERA-Interim or ERA-40 ECMWF data.

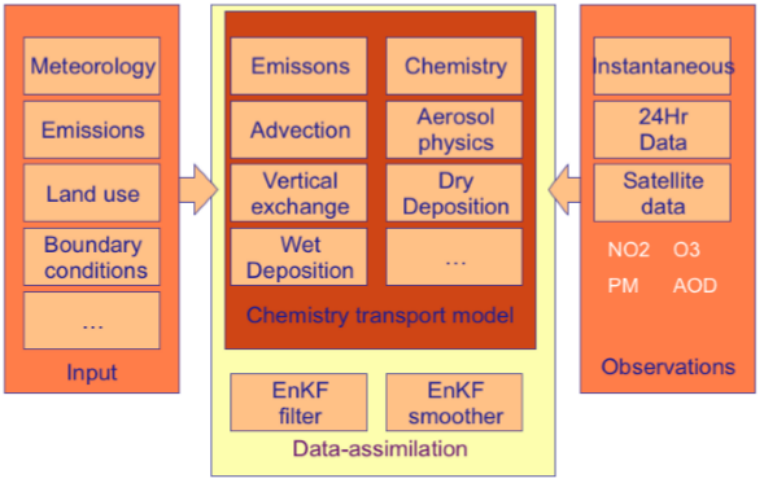

Figure 14 Schematic overview of the main building blocks of the Lotos-Euros model, including input data and observation data when used in forecasting mode.

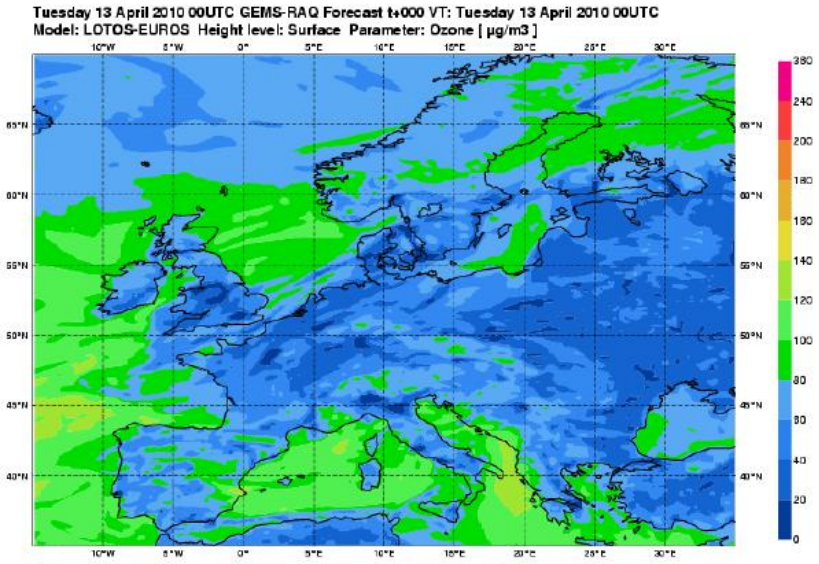

Figure 15 The default domain of LOTOS-EUROS model

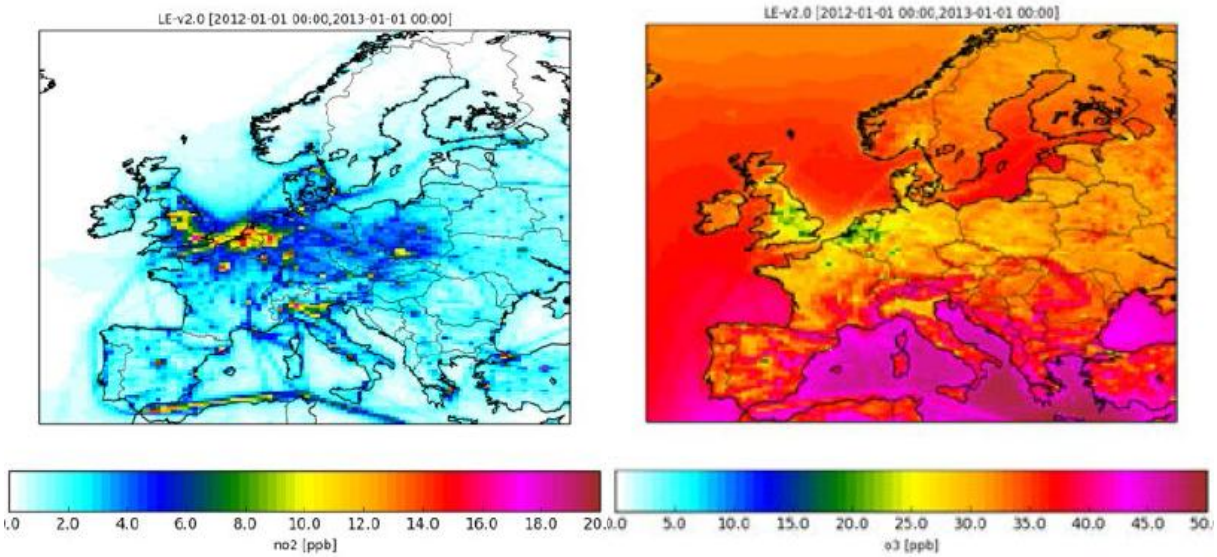

Figure 16 Results of the LOTOS-EUROS rv.2.0 model with ESCWF meteorological driver for NO2 (ppb, left) and ozone (ppb, right).

The example of spatial distribution of emissions used in the modelis presented at Figure 17.

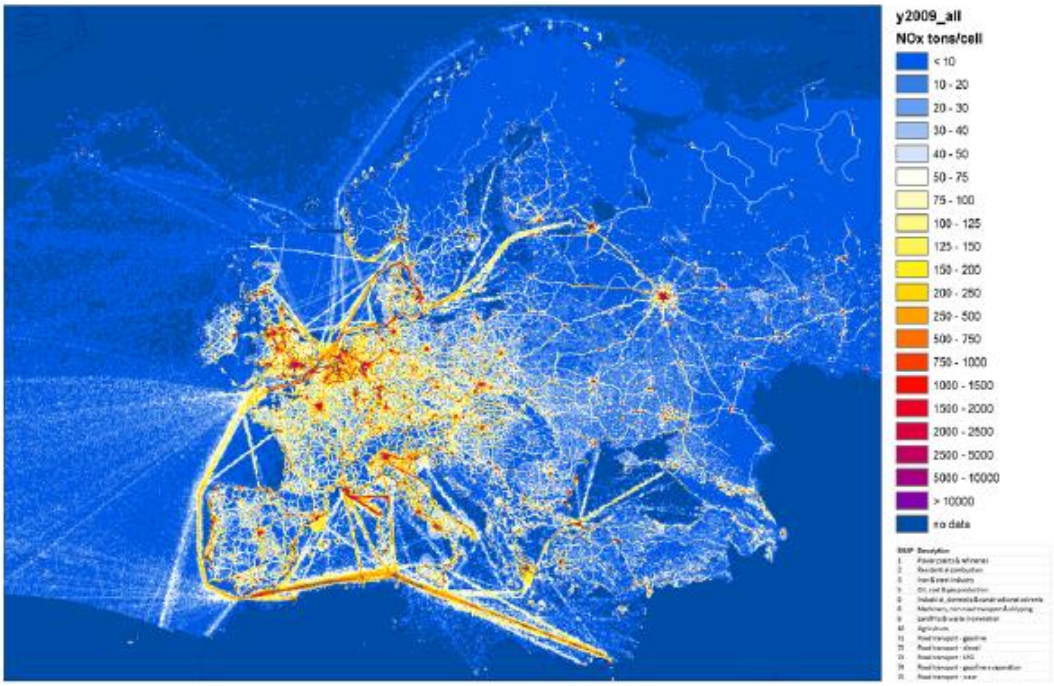

Figure 17 Spatial distribution of emissions (TNO emission inventory) for NOx in 2009.

WRF MODEL is used as meteorological driver for air quality modelling at different spatial scales. It provides input meteorological data for different applications as well as for the operational usage. It is applied in simulations of research type for two-way nested grids with horizontal resolution of 9-km, 3-km and 1-km, respectively.

HYSPLIT model. The Hybrid Single-Particle Lagrangian Integrated Trajectory (HYSPLIT) developed at the National Oceanic and Atmospheric Administration Air Resources Laboratory (NOAA ARL) is a system for computing atmospheric trajectories, complex dispersion and simulations using either puff or Lagrangian particles (Draxler 1997, 2007). The backward HYSPLIT trajectories were calculated by running the model without dispersion, thus computing the advection of a single pollutant particle within the mean wind. The gridded meteorological data fields required to run HYSPLIT were obtained from archived data sources at NCEP i.e., global latitude/longitude data from the Global Forecast System (GFS) model at 0,5° horizontal resolution. It has been applied for research purposes as well as for the identification of major emission sources influencing air pollution episodes in North-eastern regions of Croatia.

ADMS 5, advanced dispersion model used to model the **airquality impact of existing and proposed industrial installations has been installed and put to use**. Its many features include allowance for the impacts of buildings, complex terrain, coastlines and variations in surface roughness; dry and wet deposition; NO_x chemistry schemes; short term releases (puffs); calculation of fluctuations of concentration on short timescales, odours and condensed plume visibility; and allowance for radioactive decay including γ-ray dose.

ADMS-Urban, a comprehensive system for modelling air quality**in large urban areas, cities and towns has been installed and applied for several cities.** It is the only practical urban air quality model which incorporates the latest scientific understanding, explicitly represents the full range of source types occurring in an urban area, takes account of complex urban morphology including street canyons, and provides output from street-scale to urban-scale and, with the regional model link, to even larger scales.The ADMS-Urban Regional Model Link (ADMS-Urban RML) as an innovative automated system for nesting the high resolution air quality model ADMS-Urban in a regional air quality model such as CMAQ, CAMx, CHIMERE or EMEP, are using meteorological

data from the meso-scale WRF model. The output from the ADMS-Urban RML system comprises predictions of pollutant concentrations for an urban area, which take into account both regional and local pollutant transport and chemistry effects. The whole system has been installed and under further development.

ADMS-Puffmodel has been installed and used for further investigations of the instantaneous transport and dispersion of pollutants. It uses a Lagrangian puff methodology to model the fate of dense and passive gas releases. ADMS-Puff can use temporally and spatially varying meteorological data from the WRF model, or simple surface data. ADMS-Puff can also account for the impact of complex terrain: hills and variable surface roughness.ADMS-Puff calculates snapshots of instantaneous air concentration along with a time integrated dose. These concentrations can be compared against regulatory or other levels, including inbuilt flammability limits.

4.5.2.2.2. Regional climate modelling

This subsection is updated report on the DHMZ regional climate modelling activities from the year 2015. As before, the main modelling tool is hydrostatic regional climate model RegCM4 (Giorgi et al. 2012) and the use of the results from the EU FP6 project ENSEMBLES (van der Linden and Mitchell 2009) and EURO-CORDEX (e.g., Vautard et al. 2013) is still in practice.

In the rest of this subsection, we will present updated results of the evaluation of the EURO-CORDEX regional climate models' (RCM) simulations over Croatia and neighbouring countries.

Models evaluated

Three groups of models are evaluated in this report:

(1) an ensemble of ERA-Interim driven RCMs from the EURO-CORDEX initiative. These RCMs cover European domain with the minimum of the CORDEX specified domain size. Period 1989-2008 from all RCMs in this ensemble is evaluated.

(2) an ensemble of RCMs from the EURO-CORDEX initiative driven by the CMIP5 GCMs. Model period 1971-2000 (with the same historical greenhouse-gases concentrations) is used to estimate RCM performance versus observations for the same period.

(3) DHMZ set of EURO-CORDEX simulations forced by ERAInterim and CMIP5 GCMs. Two simulations forced by the ERA-Interim reanalysis are referred to as DHMZ-ERA-44 (at the 50 km horizontal grid spacing) and DHMZ-ERA-11 (at the 12.5 km horizontal grid spacing). In the GCMs-driven set of DHMZ RegCM4 simulations, four CMIP5 GCMs are also downscaled to 50 km and 12.5 km resolution (HadGEM2-ES, MPI-ESM-MR, EC-EARTH and CNRM-CM5). In 2016 the entire ensemble was recreated using alternative convection scheme (e.g., DHMZ-ERA-11-GRELL). Efforts are put at the moment to create an ensemble of projections up to the 2070 (2050) for IPCC emission and concentration scenarios RCP4.5 (RCP8.5). These results will be presented in the next report.

Observations

To evaluate near-surface (i.e., 2 meter) air temperature T2m and total precipitation amount R in previously defined sets of RCM simulations, we continue to use pan-European gridded dataset E-OBS (version 11) at the regular 0.25° grid. In this report, E-OBS will be used to estimate RCMs' performance over land, and for the two periods (1989-2008 for the ERAInterim-driven set of simulations; 1971-2000 for the GCMs-driven set of simulations).

Evaluation

Region of interest

The focus of this study is region centered over Croatia (CRO region in the rest of this paper; it covers 13°E-20°E, 42°N-47°N).

Interpolation methods

Before computing specific measures/score, different models and E-OBS observation are set to the common grids in the following manner:

(1) 0.11°/12.5 km RCMs' fields of daily T2m and R (and static topography height field) are spatially averaged 2×2 grid-cells (resulting in 0.22°/25km grids specific to each RCM), and bilinearly interpolated to the regular 0.25°×0.25° E-OBSv11 grid (now common grid to all high-resolution RCMs).

(2) 0.44°/50 km RCMs' fields of the same quantities are bilinearly interpolated to common 0.5°×0.5° grid. This common 0.5°×0.5° grid is based on EOBSv11 spatially averaged over 2×2 grid cells from the default 0.25°×0.25° grid, and these upscaled EOBSv11 fields are used to evaluate low-resolution RCMs.

(3) ERA-Interim and CMIP5 GCMs are bilinearly interpolated from their specific grids to common 0.5°×0.5° grid, and evaluated against the upscaled EOBSv11 fields.

For T2m, interpolated fields are adjusted to height difference between interpolated topography height and E-OBS topography, using free-atmosphere lapse rate of -0.65 °C/100 m.

Results

For the purpose of this report, we shall limit to evaluation of winter (i.e. DJF) spatial variability of the precipitation and 2m air temperature fields, and systematic errors through all four climatological seasons (winter/DJF, spring/MAM, summer/JJA, autumn/SON). The color- and mark- coding of all models are summarized in **Figure 18.**

Figure 18. *Color- and mark- coding of models evaluated in this report. Different color represents different boundary conditions (ERAInterim or CMIP5 GCMs) while different mark type represent different regional climate model.*

Seasonal biases

Precipitation

Mean seasonal precipitation bias spatially averaged over CRO is summarized in **Figure 19**. During winter (DJF) wet bias dominates in the most of the ERA-Interim and GCM forced RCM simulations. The effect of the alternative convection scheme (i.e. the transition from MIT to Grell (symbols with the additional black border)) is minor to moderate in 50 km DHMZ-RegCM

simulations. In 12.5 km DHMZ-RegCM simulations, precipitation biases are reduced in three out of four DHMZ GCM forced simulations. DHMZ-CNRMCM5-11 simulations is comparable to the DHMZ-ERA-11 in terms of the precipitation errors, but still all 50 km DHMZ GCM forced simulations perform better.

Larger spread of the RCMs' precipitation biases is present for the summer season. DHMZ simulations are more comparable to the rest of the EURO-CORDEX simulations, and the general impact of the convection scheme change is the reduction of the RegCM4 precipitation amounts. This changes the sign of the DHMZ-RegCM4 biases in two out of four 12.5 km simulations, increases biases in the DHMZ-HadGEM2-11 simulations, but strongly improves the performance of the DHMZ-CNRCM5-11 simulations.

In summary, although the performance of the DHMZ-RegCM4 12.5km simulations is still unsatisfactory for the winter precipitation amount, the impacts of the convection scheme change are generally beneficial for the summer precipitation amounts.

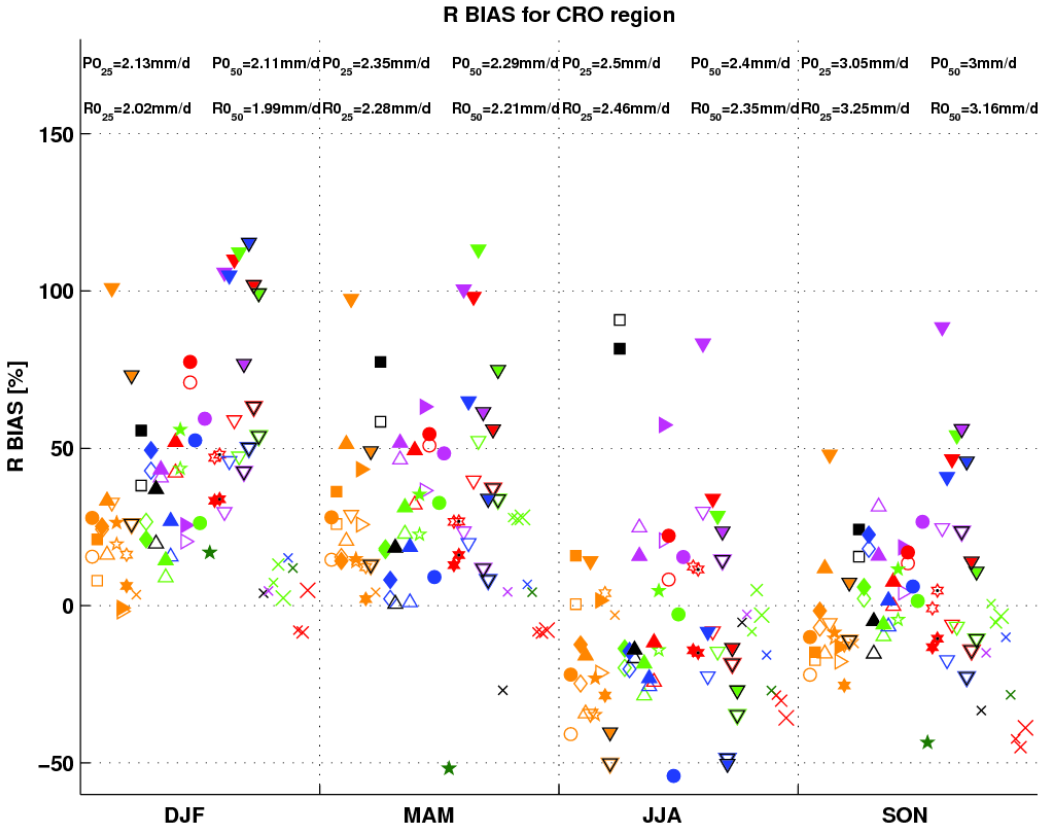

Figure 19 *Mean seasonal (winter/DJF, spring/MAM, summer/JJA, autumn/SON) total precipitation R bias averaged over CRO region (land-only) for ERA-Interim-driven and GCM-driven 0.11°/12.5 km and 0.44°/50 km RCMs and their corresponding driving global models. All GCMs and ERA-Interim are first bi-linearly interpolated to common 0.5°×0.5° grid. All units in %.*

Near-surface air temperature

EURO-CORDEX temperature errors averaged over CRO region are summarized in **Figure 20**. During winter all DHMZ-RegCM4 12.5 km are inside the spread of the other EURO-CORDEX RCMs. The convection change in DHMZ-RegCM4 12.5 km simulations introduces moderate temperature reduction in all four GCM forced simulations. This does not substantially deteriorates

DHMZ-RegCM4 12.5 km MIT simulations that have cold bias, and improves the winter temperature field over Croatia in DHMZ-HadGEM2-11 simulations. Also, the effect of the grid spacing increase is positive (i.e. the absolute T2m biases are reduced) in all MIT and Grell 50km-12.5km partner simulations.

The performance of the most of the DHMZ-RegCM4 simulations is acceptable in terms of the summer temperature biases. The contrasting pattern emerges concerning the grid spacing increase: in MIT simulations, DHMZ-RegCM4 12.5 km simulations are colder than their 50 km partners, while in Grell simulations temperature increases. During winter, both MIT and Grell simulations perform as the summer Grell simulations. This implies that the effect of the grid spacing change is related to the specific model setup and typical weather regimes (e.g., more active convection events during summer versus dominance of the large-scale weather patterns during winter over Europe).

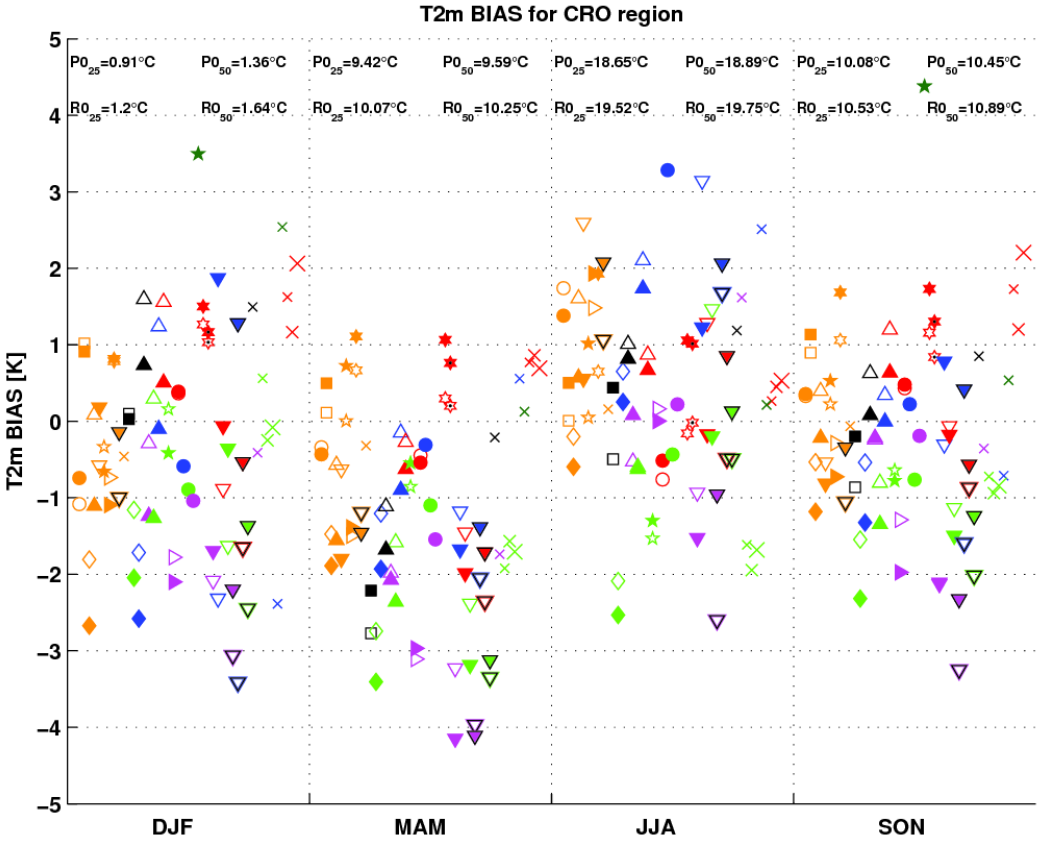

Figure 20 *Mean seasonal (winter/DJF, spring/MAM, summer/JJA, autumn/SON) T2m errors averaged over CRO region (land-only) for ERA-Interim-driven and GCM-driven 0.11°/12.5 km and 0.44°/50 km RCMs and their corresponding driving global models. All GCMs and ERA-Interim are first bi-linearly interpolated to common 0.5°×0.5° grid. All units in °C.*

Spatial variability

Precipitation

No major changes in the DHMZ-RegCM4 performance is documented compared to the 2015 report in terms of winter precipitation spatial variability (**Figure 21**). The effect of the convection scheme transition is general increase in the spatial variability in both 50 km and 12.5 km DHMZ-RegCM4 simulations, while spatial correlation coefficient is well placed in the 0.6 to 0.7 range. Although not shown, the change of the convection scheme increases spatial correlation coefficients in all four DHMZ-RegCM4 simulations, leading to values more than 0.5 when using the Grell convection scheme.

Near-surface air temperature

The variability of the mean winter and summer 2m temperature over the region CRO is summarized in **Figure 22**. Although DHMZ-RegCM4 simulations performed well already with the MIT convection scheme, the use of Grell convection scheme increase spatial correlation coefficient, leading to e.g., correlation more than 0.95 for the case of the DHMZ-CNRMCM5-11-GRELL simulation.

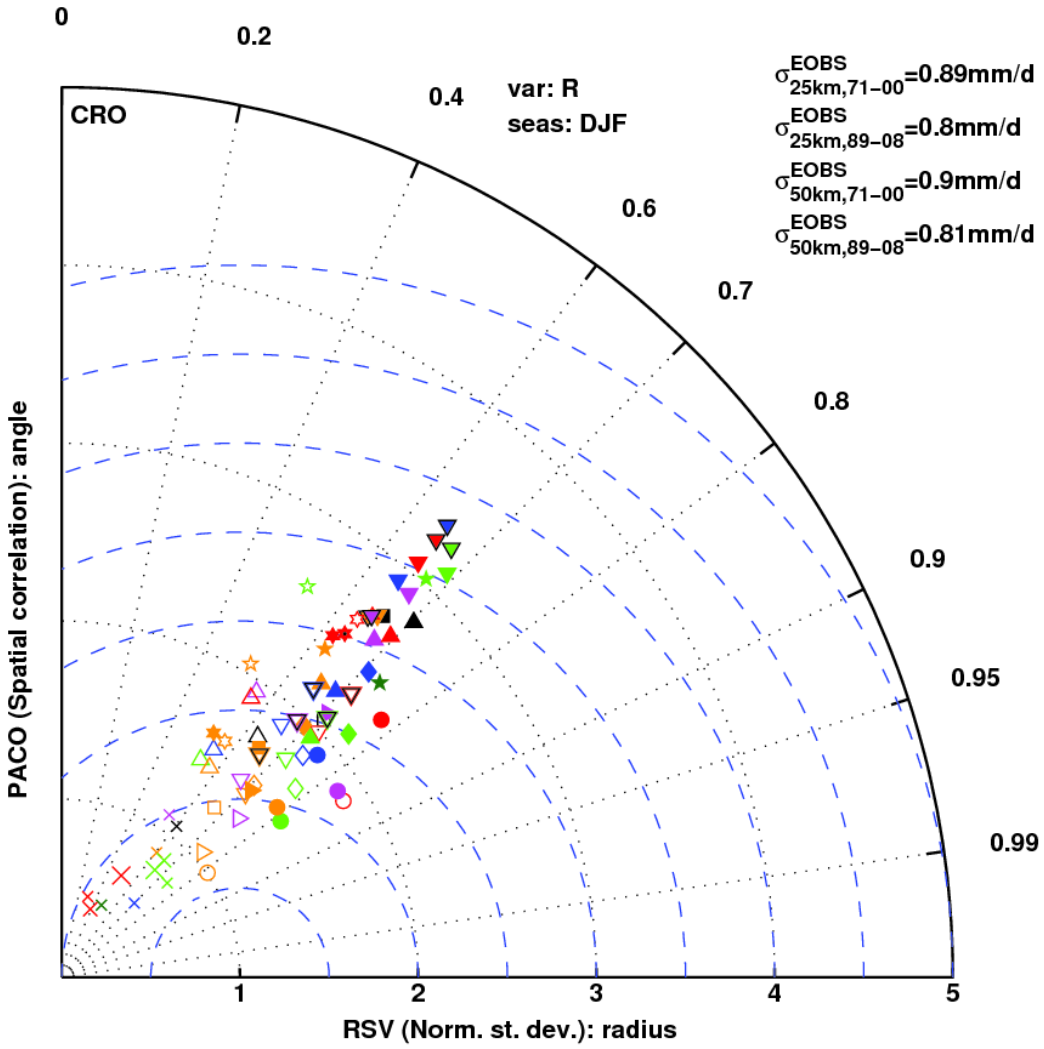

Figure 21 *Taylor diagram of mean winter total precipitation amount R in ERA-Interim and GCM-driven ensembles. RSV (the radius) is the ratio of spatial standard deviations over CRO region in RCMs (and GCMs) over E-OBSv11, and PACO (the angle) is spatial correlation coefficient over CRO region between RCMs (and GCMs) and E-OBSv11. Blue-dashed lines are centered root-mean-square differences between models and E-OBSv11 in space. In the panel left corner are relevant spatial standard deviations of the E-OBSv11 over two grids (0.25°×0.25° and 0.5°×0.5°) and for the fields averaged over the two periods (1989-2008 and 1971-2000) in mm/d.*

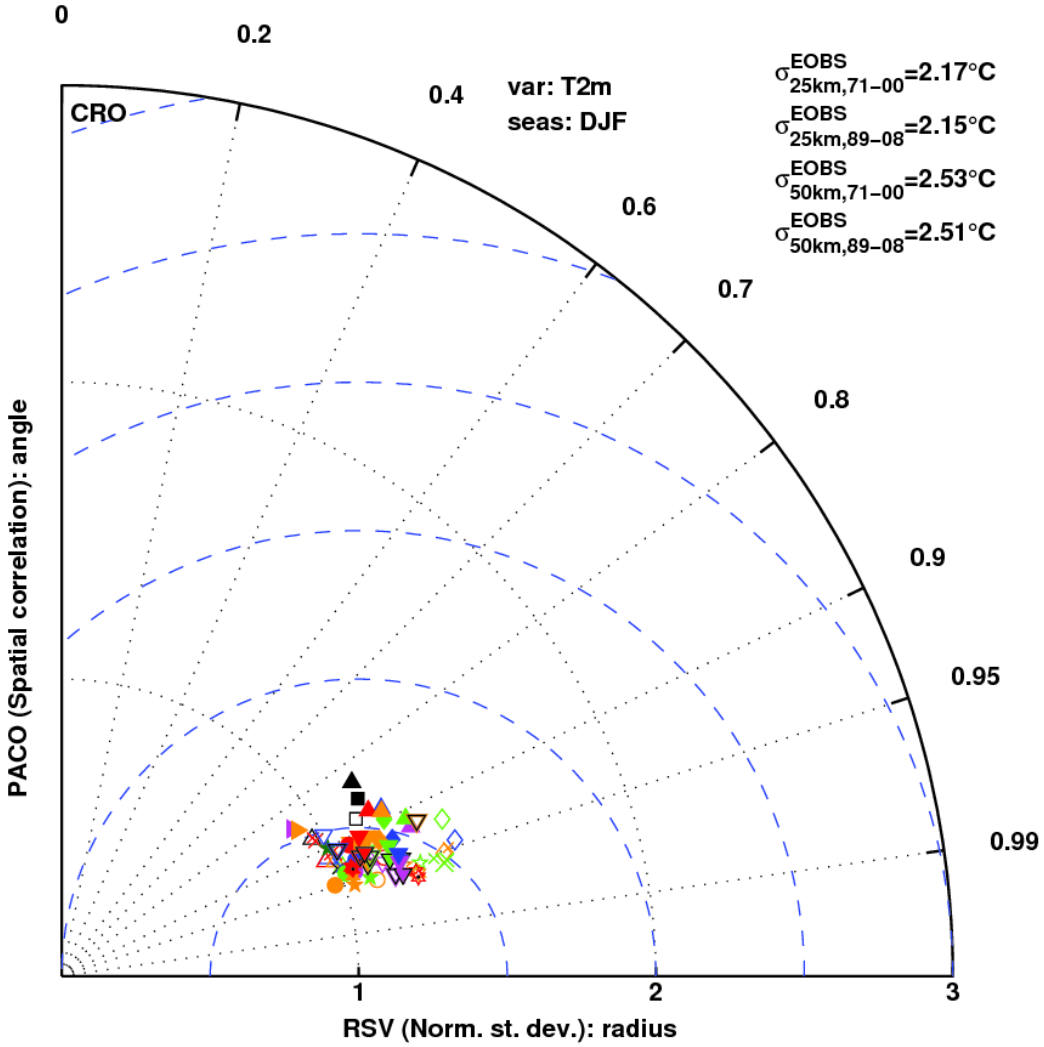

Figure 22 *Same as* ***Figure 21*** *but for the mean winter (DJF) near-surface temperature T2m over CRO.*

4.5.3 Specific products operationally available

Forecast of the road conditions. The variability of bora wind (bura) in space and time has a pronounced influence on road traffic. Therefore, knowing Bura characteristics is a necessary condition for road transport safety. To properly organize the traffic safety system, special emphasis should be given to the quality of measured long term wind speed and direction data and low resolution atmospheric forecast models.

An application, named ANEMO-ALARM (Bajić et. al., 2008), has been developed that assists road authorities in managing the traffic on the roads affected by strong wind and turbulence. The application is based on measured and forecasted wind speed and gusts for a choice of locations on Croatian roads that are most affected by severe wind. The application communicates with the user through a graphical user interface (**Figure 23**). The interface shows current and expected alarm status for road traffic safety conditions for any of the three categories of vehicles (green is for open

road, yellow for preparedness status and expected road closure and red indicated that the road is closed).

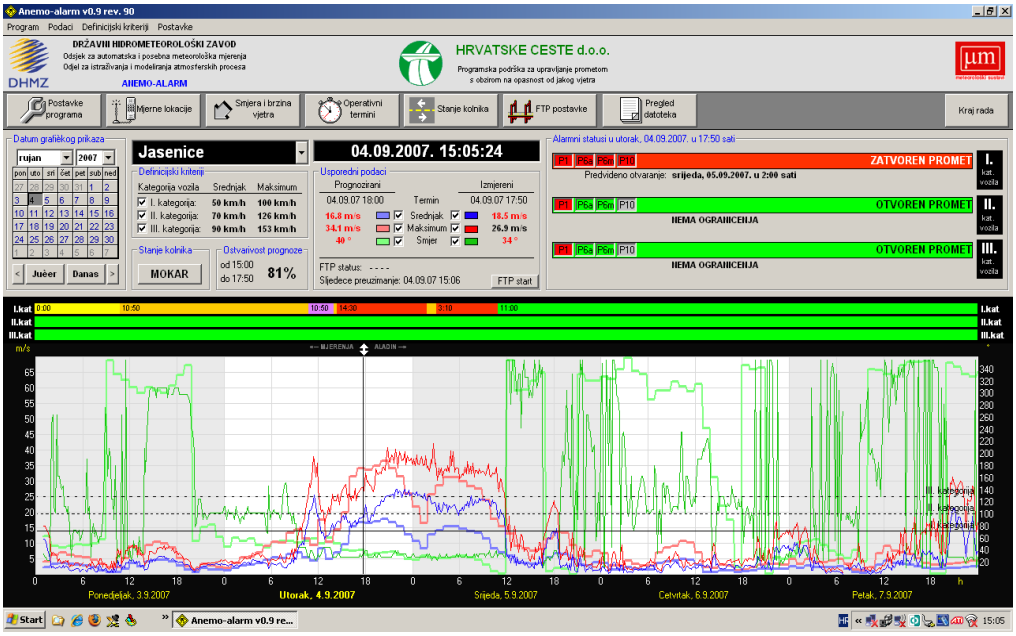

Figure 23. *The ANEMO-ALARM user interface. The measured (thick lines) and modelled (thin line) mean wind speed is shown on a graph as blue line, wind gusts are red and direction is green.*

A variety of products are prepared for energy management (transmission system operators, demand and load forecasting, distribution operators, energy traders etc.). New meteograms are developed according to the needs of partners from the energy sector.

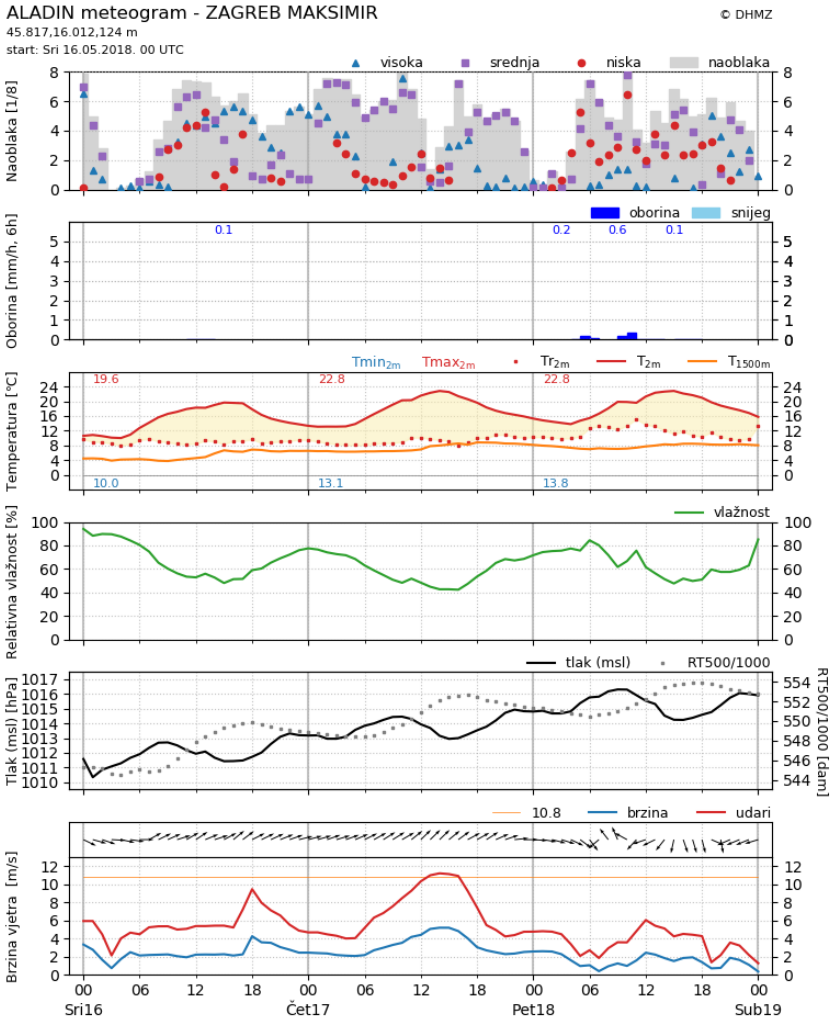

Figure 24. New meteogram using Python/matplotlib framework for partners/users from the energy sector.

4.6 Extended range forecasts (ERF) *(10 days to 30 days)*

4.6.1 Models

4.6.1.1 In operation

Locally none (ECMWF products are used).

4.6.2 Operationally available NWP model and EPS ERF products

DHMZ participates at SEECOF (South-Eastern Europe Climate Outlook Forum) which is currently leaded by SEE Sub-regional Virtual Climate Change Centre (SEE-VCCC). Seasonal forecasts for winter (December, January, February) and summer (June, July, August) are performed by consensus of NMHS representatives and end users and qualitative verification of such forecasts is made.

4.7 Long range forecasts (LRF) *(30 days up to two years)*

4.7.1 In operation

Locally none (ECMWF products are used).

4.7.2 Research performed in this field

Locally none (ECMWF products are used).

4.7.3 Operationally available EPS LRF products

5. Verification of prognostic products

5.1 In operation

In the Weather Analysis and Forecasting Department, the emphasis of the verification is put to the Department's end products (special forecasts, warnings etc.). **Figure 25** presents an example of operational (daily and monthly) real-time verification, where a comparison of maximum and minimum temperature forecasts is displayed, and basic scores are calculated. In this example a strong heat wave (followed by several weaker ones) has occurred in the beginning of August 2017, that was well predicted by the models, so end-forecasts and warnings were timely and accurate.

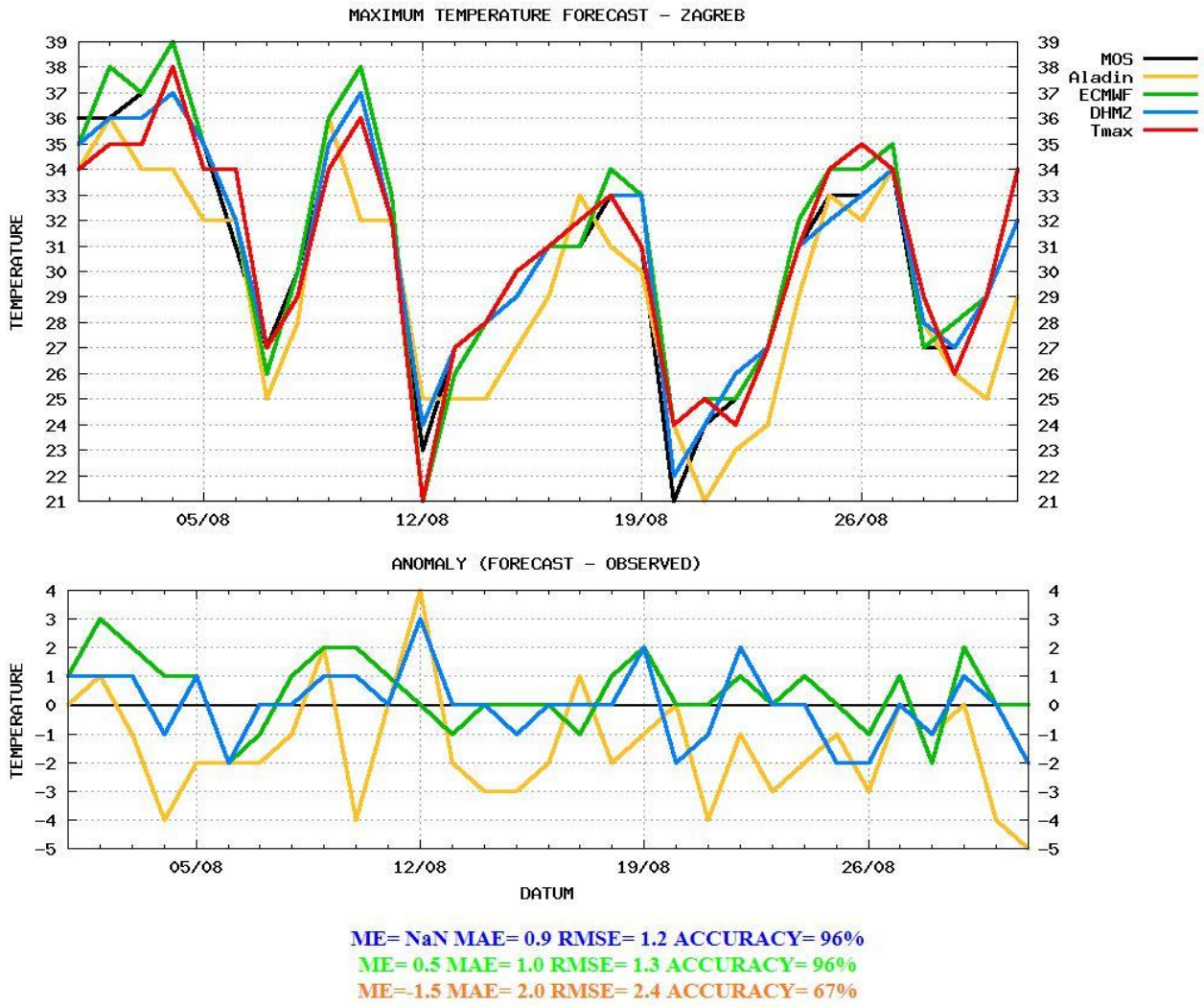

***Figure 25**. Real-time verification of 2m maximum temperature forecast (for tomorrow) for Zagreb Maksimir. for August 2017. Model forecasts (Aladin, ECMWF, DWD MOSMIX) are compared to Department's forecast (DHMZ) and observed values (Tmax). Basic scores are calculated: mean error (ME), mean absolute error (MAE) and root mean square error (RMSE). Accuracy is defined as percentage of forecasts where absolute error is less than 2°C.*

For the model verification, some ECMWF verification is carried out on a yearly basis, and results are published in Annual Report on application and verification of ECMWF products ("Green book").

Additionally, a comprehensive verification is carried out to various warnings issued by the Department, including Civil protection warnings, heat waves, cold waves, MeteoAlarm, forest fire warnings etc. **Figure 26** presents an example of heat wave warnings verification, with corresponding contingency table. Same method is applied to the verification of cold waves (introduced in season 2017/1018), and similar methods are used for other warnings systems.

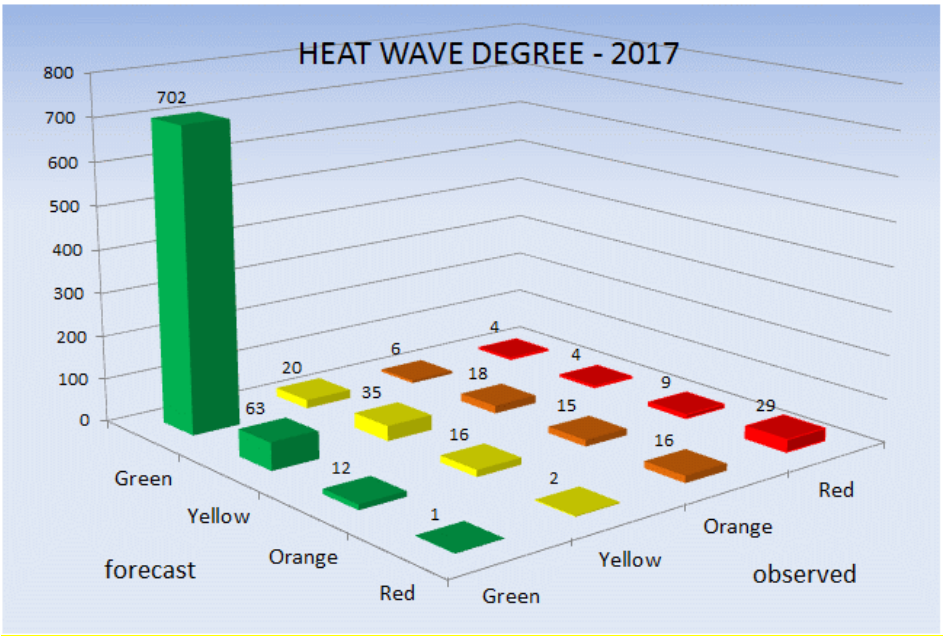

Figure 26 *Verification of heat wave warnings. Four warning levels are defined: (G)reen, (Y)ellow, (O)range and (R)ed, based on forecasted minimum and maximum temperatures for 8 Croatian regions (aggregated).Results are displayed in a graphical form representing 4x4 contingency table, with different combinations of forecasted and observed levels. Results are displayed for extremely hot season 2017, and exhibit relatively good performance of the forecasts (lead time DAY+1).*

In the Research department, standard statistical scores: RMSE, STD and bias are computed using all conventional measurements available for the data assimilation: SYNOP, TEMP, SHIP and automatic stations (Tudor et al. 2015b). Also graphs with measured and modeled meteorological quantities are produced. Operationally, Research department produces graphs of measured meteorological quantities (mean sea level pressure, 2-m temperature and humidity, 10-m wind speed, direction and gusts) precipitation and observed cloudiness together with forecasts of the same parameter obtained from various operational model forecast runs from the closes model grid point. The same is done for SYNOP and automatic stations.

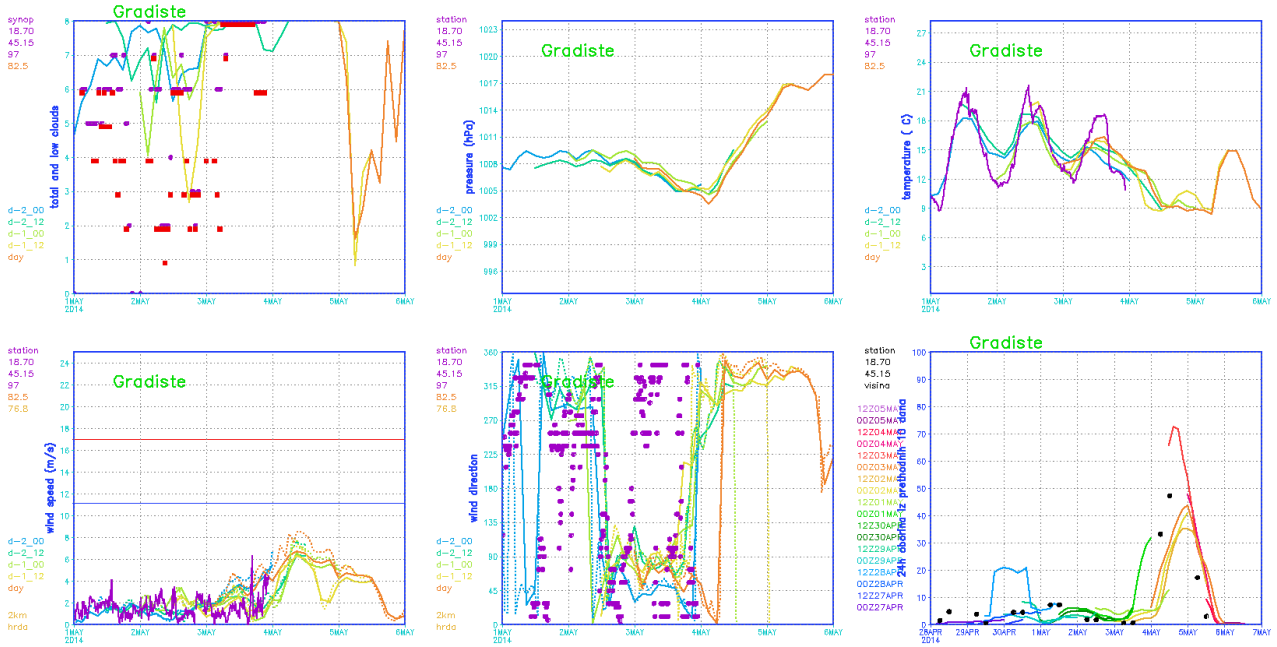

Figure 27 Measured (purple, red or black marks) and forecast from 8km (full line) and 2km (dashed) wind forecast for cloudiness, mean sea level pressure, temperature (first row) and wind speed, direction and precipitation (second row). This is an example for a SYNOP station Gradište. Details are in the text.

An example in Figure 27 shows the comparison of measured and forecast data for the Gradiste SYNOP station, the longitude and latitude and station height are shown in the top left corner of each panel. First graph in Figure 27 shows observed total cloudiness (purple marks) and low cloudiness (red marks), while other graphs at Figure 27 (except last one) show measured mean sea level pressure, temperature, wind speed and direction during the previous two days and today, as well as forecasts during the same period and the next two days. The most recent forecast run (starting today at 00) is shown in orange, yesterday's run from 12 UTC analysis is in yellow, from 00 UTC is in light green, a day before yesterday at 12 UTC is in light blue and at 00 UTC is in blue. The accumulated 24-hourly precipitation is shown in Figure 27 (last graph) for the previous 9 days, different line colors correspond to forecasts starting from different analysis times. The time of the analysis is written on the left side in the same color. The measured precipitation is shown with black dots. Similar graphs are produced automatically, every hour, after the measurements from SYNOP stations become available, for all Croatian SYNOP stations and a considerable number of SYNOP stations from the surrounding countries.

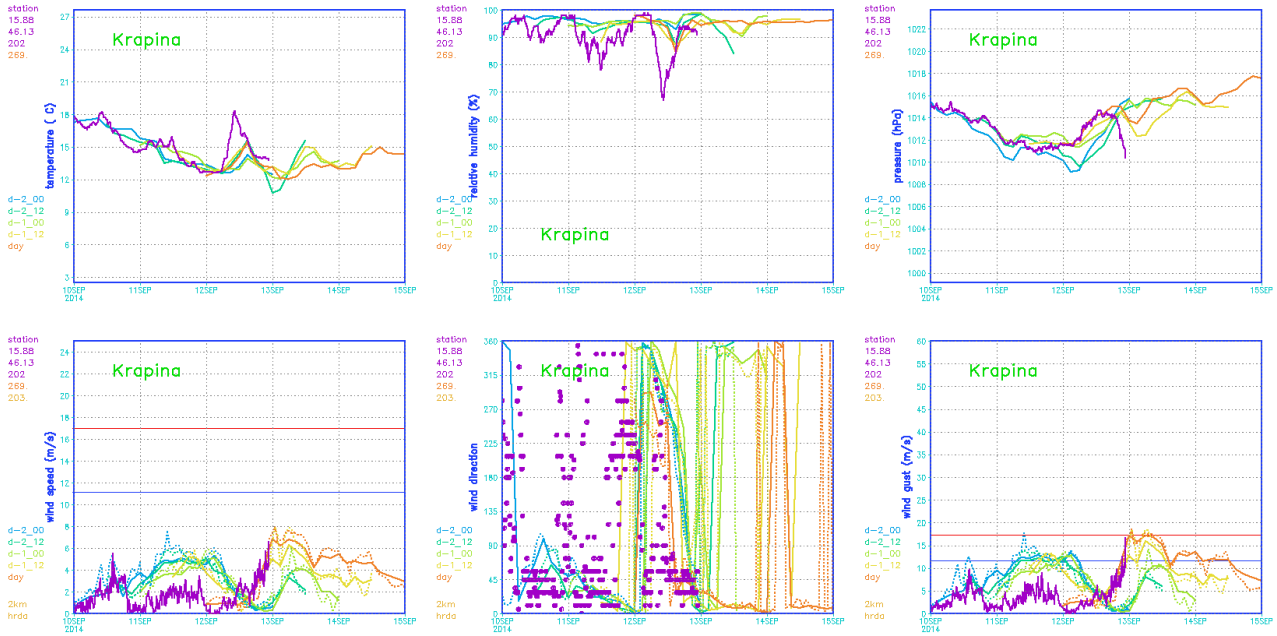

Figure 28 Measured (purple) and forecast from 8km (full line) and 2km (dashed) wind forecast for temperature, relative humidity, mean sea level pressure (first row) and wind speed, direction and gusts (second row). This is an example for an automatic station Krapina. Details are in the text.

There are more than 40 automatic stations that measure meteorological parameters in 10 minute intervals, these data are also used for operational model verification (Figure 28). This example shows the comparison of measured and forecast data for the automatic station Krapina, the longitude, latitude and height of the station are shown in the upper left corner. The comparison is made for temperature, relative humidity, mean sea level pressure, wind speed, direction and gusts. Measured values are plotted with 10 minute interval. The figures are made once per hour.

Objective verification scores are calculated against SYNOP GTS observations, Croatian automatic stations and TEMP observations covering ALADIN-HR4 domain. Temporal resolution is 6 hour for upper air verification against TEMP, 3 hour for screen level verification against SYNOP on ALADIN-HR4 domain and 1 hour for the verification against only Croatian meteorological stations on area of Croatia. One example of such plots is shown at **Figure 29**.

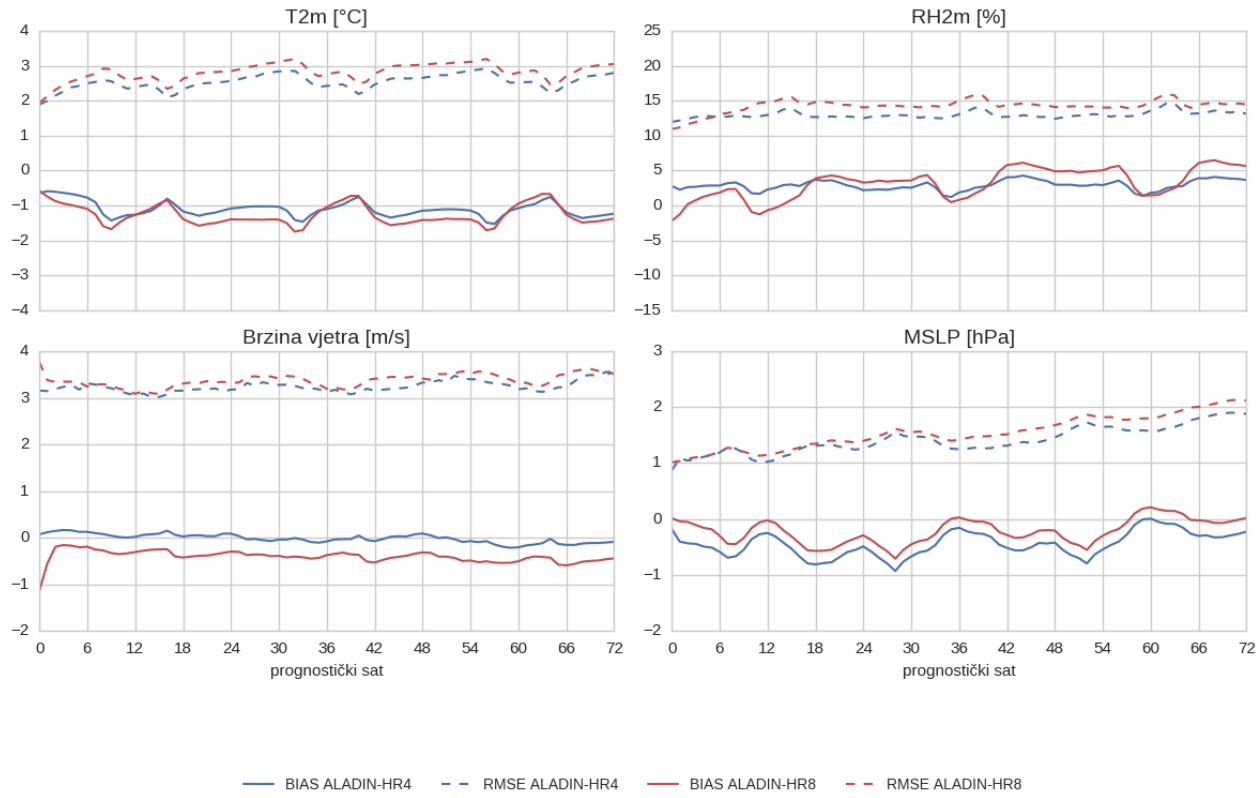

Figure 29. *BIAS and RMSE against lead time for two ALADIN configurations. Scores were calculated over one month (January 2017) and observations used are from local Croatian meteorological station network.*

Additionally, number of scores based on contingency tables is calculated such as frequency bias, hit rate, false alarm ratio, false alarm rate, threat score, the equitable threat score…

Except local tools a verification tool developed in ALADIN community, called VERAL (verification for ALADIN, http://www.rclace.eu/File/NWP_Utility_Inventory/ ALADIN/Czech Republic/quest_CHMI_veral.doc) is installed at DHMZ and is used for operational verification as well as testing of new versions of model code available for operational forecast and various options and tunings before a new model version is introduced to the operational forecast suite. The VERAL program package produces standard deviation, bias and root mean square error of surface variables, such as 2m temperature and relative humidity, mean sea level pressure, wind components as well as wind speed and direction. It also computes the same statistical parameters in vertical-time cross sections for temperature, geopotential height, wind speed and direction and relative humidity on standard isobaric surfaces using vertical soundings available over the model domain.

Additionaly, HARMONIE verification package (Yang, 2008) has been ported locally. The operational forecast data are also sent to the joint centre for verification using the same package, so this also enables inter-comparison of model forecasts from different services (and hence different models, model versions, options, resolutions etc.). This verification package is more advanced and computes more scores when compared to VERAL and offers more flexibility.

Verification is performed using standard GTS data available via global exchange and high - resolution in - situ data from the national network (when possible). The measurements used for verification by the common tools such as the HARMONIE package mentioned previously are obtained from ECMWF, where the measured data are quality checked, flagged and discarded by an automatic procedure. Unfortunately, this means that some measured data during particular weather phenomena are discarded as wrong.

The performance of the operational forecast can be monitored on the intranet where the recent and historic products of the VERAL verification package can be accessed. The scores are computed

monthly, seasonally and separately for cold/warm part of the year. The scores are computed for both surface and upper air fields, regularly after the period of interest finishes. The verification products for the operational forecast computed using HARMONIE verification package are also available via intranet where a practical user interface allows a choice in the variable and score to be displayed.

Subjective verification of precipitation: Subjective verification of precipitation is based on comparison of figures of 24h accumulated precipitation fields over ALADIN-HR2 from ALADIN-HR2/HR4/HR8 models with precipitation figures of measured precipitation. One example of such subjective verification is shown on **Figure 30**.

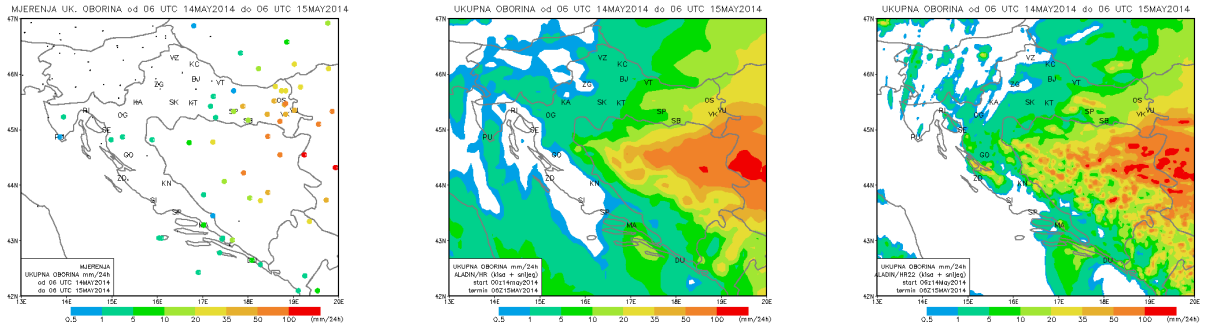

Figure 30. *24h accumulated precipitation from measurements from rain gauges (circles) (left), 8 km forecast (middle) and 2 km forecast (left) for 20140514 06 UTC – 20140515 06 UTC.*

5.2 Research performed in this field

Ongoing work on wind speed and direction verification including RMSE decomposition and quantitative spectral verification (Horvath et al., 2012) was extended to more stations from different climate regions of Croatia. Verification of operational 10 m wind forecast obtained from ALADIN mesoscale numerical weather prediction model was performed for ALARO 8 km (AL8) and simplified DADA 2 km (DA2) models, with the addition of forecasts from non-hydrostatic ALARO 2 km (AL2) model. AL8 and DA2 forecasts were initialized daily at 0000 UTC and driven with the ARPEGE global model forecasts through the 72-hourly forecasting range with the 3-hourly interval of data availability, while AL2 model was initialized from 0600 UTC AL8 forecasts and run through the 24-hours forecast range with the 1-hourly interval of data availability.

The results of RMSE decomposition showed that RMSE values are largest at bora dominated coastal stations (bo) and significantly decrease at coastal stations with significant portion of thermally driven flows (th). RMSE values are smallest within third group (hi), composed of highland valley and mountain foothill stations. As RMSE is generally proportional to wind speed this feature is quite expected, as well as the fact that RMSE is generally highest during winter and smallest in summer. Increase of ALADIN horizontal resolution significantly decreases RMSE at ‘bo’ group of stations, while the improved model setup (complete physics and non-hydrostatic) at higher resolution had significant effect on RMSE only at ‘th’ group of stations. The largest portion of RMSE errors can be attributed to phase errors (PHE), except maybe for AL8 model at bora dominated stations where bias of the mean (BM) has similar or even greater contribution. With the

increase of model resolution BM and bias of the standard deviation (BSD) generally decrease, while the PHE increases.

The quantitative spectral evaluation of wind components was performed in the frequency domain. Entire spectral range was separated in the following three bands: larger than diurnal (LTD; 26 hours < T < 7 days), diurnal (DIU; 22 hours < T < 26 hours) and sub-diurnal (SUB; 6 hours < T < 22 hours). Within the evaluation procedure we consider the share of spectral power (observed or modelled) in different spectral ranges normalized by the total power (observed or modelled), as well as the ratio of modelled and observed power within individual spectral range. If the first one would be the same for both the model/observations and the second equals one, then we would have an ideal modelled spectra. In order to test the efficiency of our models in simulating observed spectra for different types of stations, we have made a scatter plot with the above mentioned two spectral features on coordinate axis (**Figure 31**). If we first focus on observations and variability along x-axis, we clearly see that totally 12 stations can be classified into three groups. On the other hand, neither of the model data does not display such a difference between various groups of stations. Generally, with increasing the model horizontal resolution and then its complexity at finer resolution, the share of power within individual ranges becomes closer to observations. This is especially the case for the 'bo' group of stations and somewhat less for the others. Generally, the shares are poorly represented for 'hi' group of stations. Now we shall focus on the ratio of modeled and observed spectral power within individual spectral ranges (y-axis, **Figure 31**). We can see that this ratio is mostly underestimated by AL8 model in LTD and SUB ranges for 'bo' group of stations, as well as in LTD range for 'hi' stations. Both higher resolution models overestimate this range in all ranges and for all group of stations, i.e. their spectra are shifted upwards along y-axis, or more precisely they have more realistic share of power within individual ranges than AL8, but the total amount of power in the system is overestimated.

Finally, we have made some effort to link the results of statistical and spectral verification, i.e. we have tried to find how different contributors to RMSE affect the model ability to represent observed spectra. Preliminary results have shown that the along y-axis shift of modeled spectra (overestimation of total spectral power) is significantly related to BSD, where negative BSD is related to downward shift and positive BSD to upwards shift of modeled spectra. The correlation is very strong, and does not depend on the model resolution or type of the station. On the other hand, the model ability to represent the proper share of spectral power in different spectral ranges does not show such a strong link to any of the RMSE components, except for the 'bo' group of stations which is the most homogeneous of all groups. Despite similar spectral characteristics, shares of RMSE components differ for all other groups which weaken the correlation.

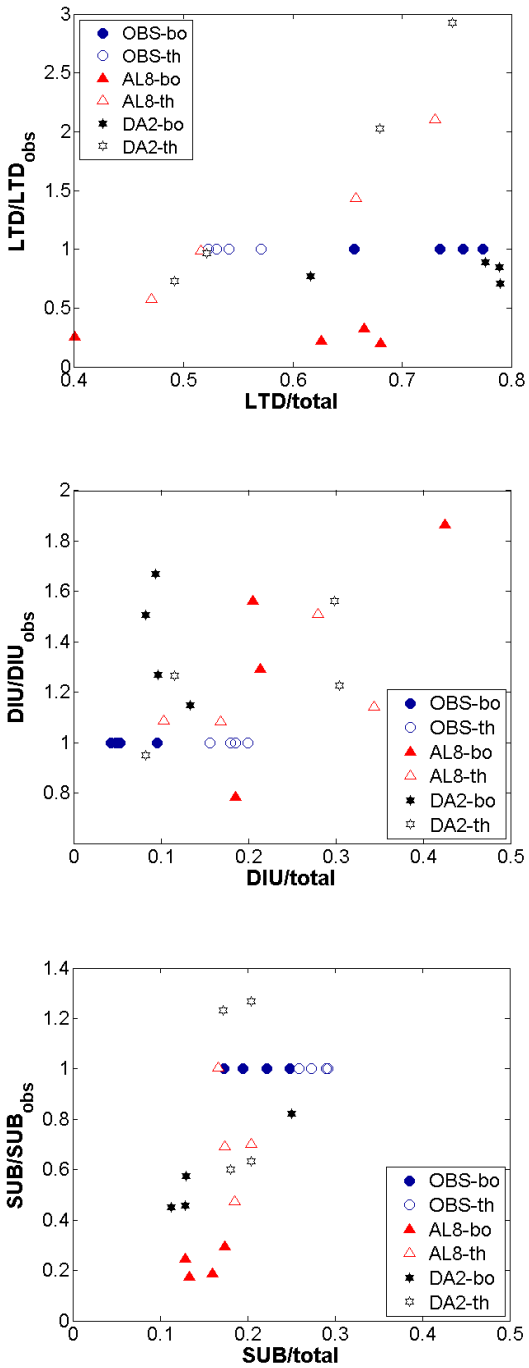

Figure 31. *The spectral power distribution of cross-mountain wind component (measured or modeled) in different spectral ranges normalized by total power (measured or modeled; x-axis) and by the observed power in the same spectral range (y-axis) at the same station.*

6. Plans for the future *(next 4 years)*

6.1 Development of the GDPFS

6.2 Planned research Activities in NWP, Nowcasting and Long-range Forecasting

According to the results of testing over a three year period in complex terrain of Croatia, the analogue-ensemble post-processing method increases the accuracy of the wind speed predictions of the current NWP operational system. Further research is needed, especially in the area of extreme winds. If the methods provides useful for extreme winds, it will be tested operationally.

6.2.1 Planned Research Activities in NWP

In data assimilation we intend to test different procedures for obtaining B matrix and impact on forecast and to include new observations in data assimilation (Radar data, GPS…).

Further research in post-processing methods will focus on analogue ensemble and Kalman filtering for wind speed and solar irradiance forecasting. This will include forecast uncertainty estimates derived with analogue ensemble method. It is expected that these methods will become quasi-operational in near future.

Improved representation of surface in the forecast model through improved sea surface temperature (SST) and physiographic fields (topography, roughness length, soil types).

For the wave model following improvements are considered:
- We need better parameterizations. One key is the Ardhuin et al (2010) formulation, but which depends on many parameters.
- We always need better wind model output to get better wave forecasts.
- We need to improve the speed of the model.
- We need better grid for the model runs.
- We need comparison with wave buoys which provide the most reliable way to access wave data, and the only way to get data besides significant wave height.
- Also interesting is coupling of wave model with atmosphere (for exchange of Charnock coefficient) and circulation (for getting currents)

Different version and configurations of the ALADIN model are planned to be tested on horizontal grid spacing smaller than 2 km, which is currently the highest resolution being operationally applied at DHMZ

6.2.2 Planned Research Activities in Nowcasting

Planned activities include installation of the new version of the NWC SAF software and evaluation of the products in the local environment. Additionally, MPEF GII (Global Instability Index) products will be evaluated and development of the combined forecast instability index, based on the evaluation using lightning data, is planned.

Further work on wind nowcasting and ultra-short range forecasting up to 3 hours lead time with 10-min interval is planned to finalize the research results and implement the system quasi-operationally into the ALADIN forecast system at DHMZ.

For nowcasting, INCA precipitation module will be implemented, using OPERA datacentre Odyssey instantaneous surface rain rate radar composites and automatic rain gauge network. Verification of INCA nowcasting fields will be made.

6.2.3 Planned Research Activities in Long-range Forecasting

7. Hydrological / hydraulic modelling and hydrological operational forecasting system (HOFS)

7.1. Introduction

National Meteorological and Hydrological Service of Republic Croatia (DHMZ), Hydrology division, uses three different hydrological models: Sava Super model (Sava SM) in Croatia and Bosnia and Herzegovina, European Flood Awareness System (EFAS) and WMO South East Europe Flash Flood Guidance System (SEEFFGS).

7.2. Models

7.2.1. Sava SM in Croatia and Bosnia and Herzegovina

DHMZ and Croatian Waters (HV), mutually developed hydrologic/hydraulic 1D/2D model of Sava catchment in Croatia and Bosnia and Herzegovina from the Slovenian border until Serbia with DHI/Proning as consultants. It was done within period September 2014 - December 2016 in two phases. The first phase lasted September 2014-September 2015 and covered Kupa and Upper part of Sava River to the confluence at Sisak Town, including tributaries to that two rivers. The second phase lasted December 2015-December 2016 and covered the rest of Sava catchment in Croatia but also in Bosnia and Herzegovina. During the first phase of HOFS development we covered 10533 km^2 or cca 19 % of Croatia, and during the second phase we covered 13709 km^2 or cca 24 % of country, that is finally 43% of Croatian teritory.
The Sava SM model was built within MIKE11 software (DHI). It is operational, runs regularly at hourly frequency at DHMZ on a PC.

7.2.1.1. Equipment in use for the hydrological operational forecasting system (HOFS)

The computer used for the HOFS is a PC HP ProDesk 490 G2 MT with Intel Core i7-4790 CPU 3,6 GHz and 8 GB RAM. It runs in Win 7 Professional on 64 bit. The storage is on internal HDD of 15 GB. The model runs in MIKE11 software (DHI) and DHMZ has 2 network and 2 single licenses. The hard key (dongle) for operational Sava SM it is installed on Hydrology division's PC.

7.2.1.2. Hydrological operational forecasting system (HOFS)

A combined hydrological-hydrodynamic MIKE11 model has been developed partly based on the existing hydrodynamic sub-models, existing upstream sub-models developed jointly with Agency for Environment (ARSO) in Slovenia and new hydrological sub-models which have not been already modelled. After development and calibration of the MIKE11 model, the model has been upgraded to a forecasting model, which is applied in the operational flood forecasting system. The final forecasting system has been installed at DHMZ and at Croatian Waters (HV), where it is possible to run additional flood control scenarios. The forecast are issued automatically each hour for the next 4 days.
During the first period of 12 months, an operational flood forecasting system has been developed for the Kupa and Upper part of Sava River to the confluence at Sisak Town, including tributaries to these two rivers. The forecasting system provides forecasts of water level and discharge on 43 river locations, for the next 4 days.
During the following (second) period of 12 months we continued our work and developed HOFS for the rest of Sava catchment within Croatia and for transboundary river Una (between Croatia and Bosnia and Herzegovina), but also for the main Sava's tributaries in Bosnia and Herzegovina (Vrbas, Bosna, Tinja, Ukrina) as a rough inflow. **The final model is named Sava SM and it provides forecasts of water level and discharge on 145 river locations, for the next 5 days.**

The forecasting system is synchronized with a similar Slovenian flood forecasting system at ARSO including real-time exchange of inflow forecast and online data. The HOFS is completely automated and provides a new forecast each hour with a total execution time of 10 minutes. All forecasts are disseminated to a WEB page where it is possible to monitor flood warning status for the next 5 days on a map, on charts, in tables and in reports.
The HOFS is a Cloud based forecasting system, which has been installed physically on a PC at DHMZ's premises, but can work from any location. After the forecast simulation is completed, the model behind the forecast simulation with all real-time data is made available in the cloud ready for further processing. When required, it is possible to make further analysis of the forecast, including simulation of various flood control scenarios. Provision for simulation of these scenarios has been made operational on computers at both HV and DHMZ.
The HOFS with MIKE11 is based on the real-time data received from available online hydrological and meteorological stations in Croatia, Slovenia and Bosnia and Herzegovina, relevant hydrological forecast from Slovenia and prediction from the meteorological models ALADIN and ECMWF as shown at the **Figure 32**.

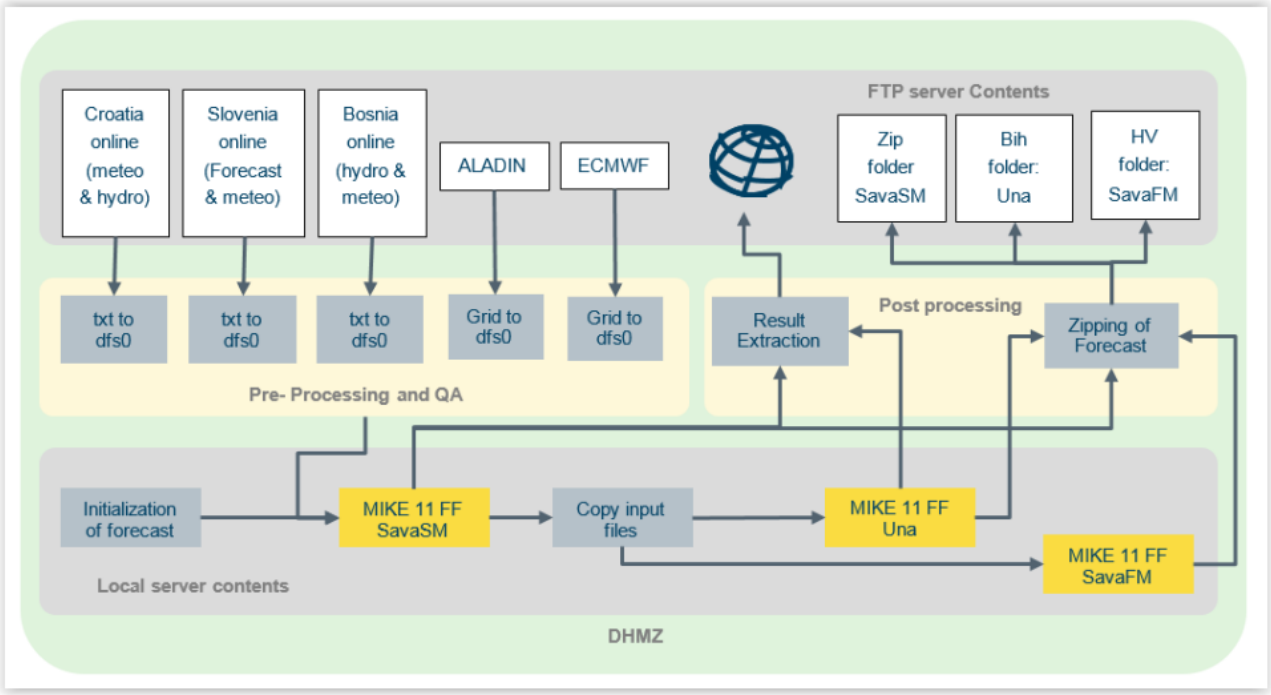

Figure 32 *Automated flood forecasting sequence (systems flowchart).*

The automated system runs each hour using the following steps:

1) Firstly, all online data required for making a flood forecast are collected on a FTP Server located at DHMZ. The online data includes data form the Hydro-Meteorological Telemetric Network (collected from DHMZ online database), online data and inflow forecast from Slovenia (prepared and uploaded by ARSO in Slovenia), online meteorological and hydrological data from Bosnia and Herzegovina (prepared and uploaded by two federal Hydrometorological services of BIH from Sarajevo and Banja Luka, and by the Agency for the Sava River Basin from Sarajevo) and prediction from the Meteorological Models: ALADIN and ECMWF (prepared by meteorologists at DHMZ).
2) When all online data are ready on the FTP server, data are downloaded for further processing and control before the time series can be applied in MIKE11.

3) The Forecast simulation takes place as a batch job running MIKE11, initialized each hour to start a MIKE11 simulation, which is performed as a so called hot-start run using conditions form the previous simulation.
4) After the forecast simulation is completed, results are extracted and uploaded to a web page.
5) Based on input files from the full model simulation, the automated forecasting system also includes forecast simulations of Una model.
6) Finally, the completed model setup including time series is compressed into a zip-file and uploaded to the FTP Server, which makes it possible to run scenarios using MIKE Operations at any location.

The automated system is scheduled to run every hour, and is prepared as one complete batch job which run a sequence of all jobs required in the 5 step procedure described above. The complete sequence of batch jobs (total 20 jobs) is normally executed within 15 minutes.

Results from the forecast simulation are uploaded to a Web Page as shown below in **Figure 33**.

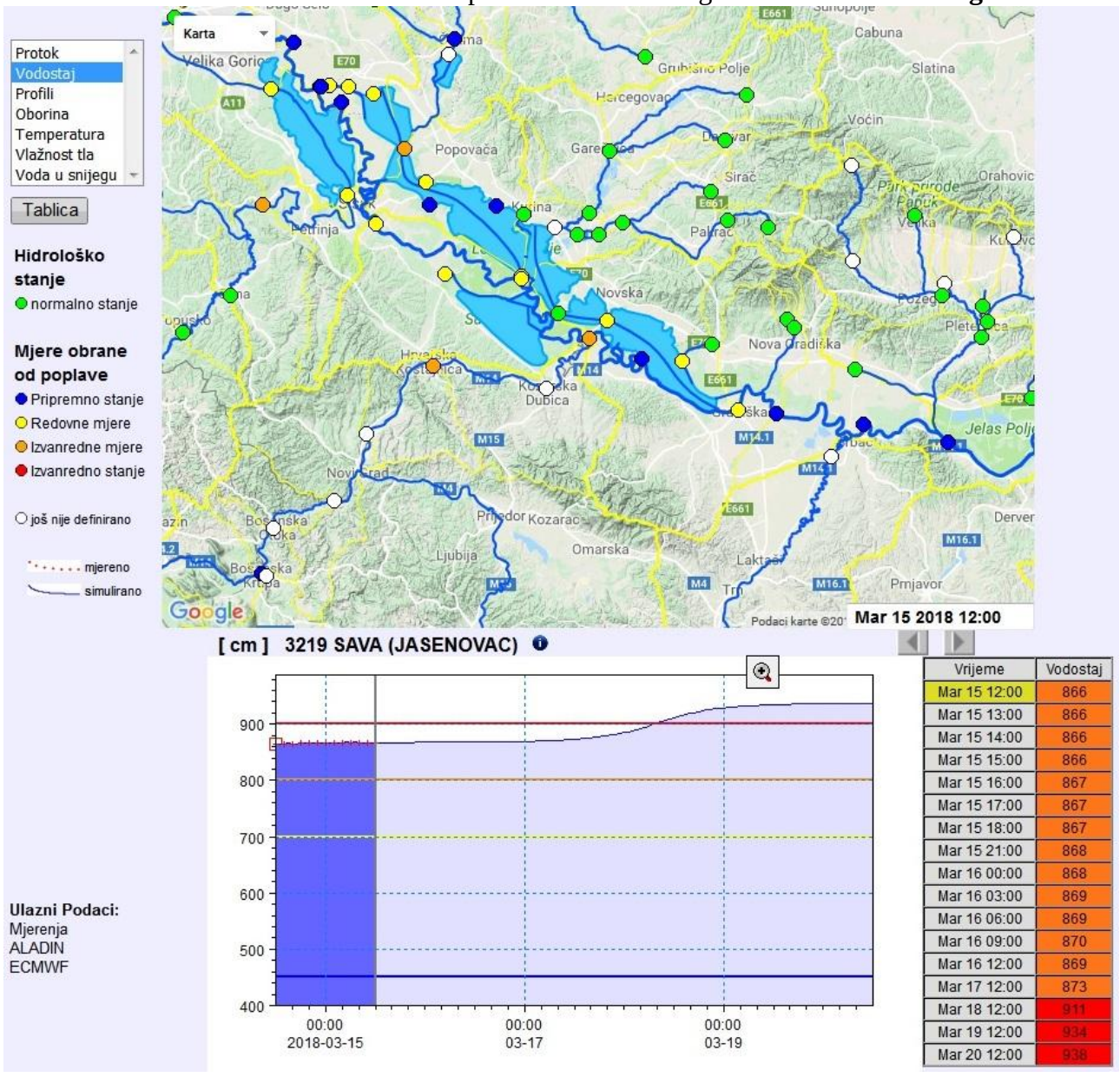

Figure 33 *Screen dump of forecasting web page for forecast dissemination, an example of March 2018 flood*

The WEB page gives presentation of 6 data types including:

- Discharge
- Water level (also presented within a river profile)
- Precipitation
- Temperature
- Moisture content in root zone
- Snow depth (water equivalent)

Each data type has been colour coded showing thresholds of warning levels (used for discharge and water levels) or coloured according to the size of values (used for other data types). Time series for each station or sub-catchment are presented on charts and tables when clicking on the map. In addition all data are presented in reports for each data type.

7.2.1.3. Development of the DHMZ's HOFS

We continue to develop the Sava SM HOFS with updating of new meteorological models inputs, ensembles, etc.

7.2.2. European Flood Awareness System (EFAS)

From the year of 2013 DHMZ as a partner joined the EFAS and started to prepare and send data to it. It runs in ECMWF in two different models-one for fluvial (river) flooding and the second one for the flash flooding. The EFAS Partnership gives the Partner real-time access to the EFAS products through the EFAS Information System (EFAS-IS).
EFAS is the first operational European system monitoring and forecasting floods across Europe. It provides probabilistic, flood early warning information up to 10 days in advance to its partners: the National Hydrological Services and the European Response and Coordination Centre (ERCC).
The Operational EFAS consists of four centres executed by different consortia:

- **EFAS Computational** centre - European Centre for Medium-Range Weather Forecasts (UK) executes forecasts and hosts the EFAS-Information System platform
- **EFAS Dissemination** centre - Swedish Meteorological and Hydrological Institute, Rijkswaterstaat (NL) and Slovak Hydro-Meteorological Institute analyse EFAS on a daily basis and disseminate information to the partners and the ERCC
- **EFAS Hydrological data collection** centre - REDIAM (ES) and ELIMCO (ES) collect historic and realtime discharge and water level data across Europe
- **EFAS Meteorological data collection** centre – KISTERS AG and Deutscher Wetterdienst collect historic and realtime meteorological data across Europe.

EFAS is an operational service under the umbrella of the Copernicus emergency management service and is fully operational since October 2012.

Ensemble Prediction Systems

EFAS uses multiple weather forecasts and EPS as input. Its forecasts are based on two deterministic, medium-range forecasts from the European Centre for Medium-Range Weather Forecasts (ECMWF) and the German Weather Service (DWD), (and thus different models) and on two sets of EPS: One from ECMWF which covers the medium-range up to 15 days globally (with a spatial resolution of ~30 km and 51 members, and one from the Consortium for Small-scale Modelling (COSMO), a limited area model EPS covering most of Europe with a shorter range up to 5 days (with a spatial resolution of 7 km and 16 members). The reason for using the shorter term EPS is to enhance the spread of EPS within the first few days and to have finer grid information in

particular for mountainous areas. This allows to better identifying the location of the floods within the river basin.

LISFLOOD – the hydrological model for EFAS

The hydrological model used for EFAS is LISFLOOD. The model is a hybrid between a conceptual and a physical rainfall-runoff model combined with a routing module in the river channel. LISFLOOD has been specifically designed for large river catchments. A particular feature of LISFLOOD is its strong use of advanced Geographical Information System (GIS), in particular as a dynamic modelling framework.

Reducing false alarms – threshold exceedance and persistence

EFAS is providing information to the national hydrological services only when there is a danger that critical flood levels might be exceeded. In EFAS, the critical thresholds are needed at every grid point and therefore cannot be derived from observations. Instead, based on observed meteorological data, long term discharge time series are calculated at each grid with the same LISFLOOD model parameterisation that is set up in the forecasting system. From these long-term simulations return periods are estimated – currently the 1, 2, 5 and 20-year return periods. All flood forecasts are compared against these thresholds – at every pixel – and the threshold exceedance calculated. Only when critical thresholds are exceeded persistently over several forecasts, information at these locations is produced, e.g. in the form of colour-coded overview maps or time series information at control points. The persistence criteria has been introduced to reduce the number of false alarms and focus on large fluvial floods caused mainly by widespread severe precipitation, combined rainfall with snow-melting or prolonged rainfalls of medium intensity.

Verification

Forecast verification is important to understand the strength and weaknesses of the system and to build confidence in its results. For EFAS two types of verifications are applied. The first one is event-based – for each flood alert the hit, false alarm and misses are assessed. If a flood alert has been sent but no flooding was observed, a false alarm is counted. If somewhere in the basin flooding has been report, a hit is counted. If flooding has been reported for which an alert was not sent (even if the system itself simulated an event), a missed event is counted. The events are assessed through feedback reports and media throughout the year and reported during the EFAS annual meeting. In addition to the event-based verification, also skill scores are computed including Brier Skill Score, Root Mean Square Error, Nash Sutcliffe efficiency, continuous rank probability score, etc. These are reported regularly in the EFAS bulletins and in publications. More on skill scores can be found on HEPEX.

Seasonal outlook

The seasonal hydrological outlook is calculated from the current seasonal forecast (produced by forcing the LISFLOOD model with the 51 members ensemble from the ECMWF System 5 seasonal forecast) with respect to the 90th and 10th percentiles of the simulated discharge from a 24-year model climatology run (1990 - 2013). The seasonal forecast outlook plots are updated on a weekly basis with the latest weekly averaged water balance. A new seasonal forecast outlook (map and plots) is generated at the beginning of each month when the new forecast becomes available (usually on the 8th of the month).

7.2.3. Flash Flood Guidance System (FFGS)

At the XV congress of the WMO in 2007, it was decided to establish a Flash Flood Guidance System program worldwide. Flash Flood Guidance System was developed and is being implemented by HRC (Hydrologic Research Center, San Diego, USA) and financed by USAID/OFDA in collaboration with NOAA/WMO.

Flash flood global coverage concept plan is to eventually establish a series of regional centers, which will provide flash flood related products and support services to their respective regional participating country National Meteorological and Hydrologic Services (NMHSs). Using those products, NMHSs can provide flash flood watches and warnings to their own national agencies like emergency management authorities, municipalities, and water resources agencies. Meeting for the establishment of a Flash Flood Guidance System for South East Europe (SEE) was held in Ankara, Turkey on 22-24 January 2013. Croatia, Serbia, Slovenia, Romania, Bosnia-Herzegovina, Macedonia, Moldova, Albania and Montenegro as well as Turkey, WMO, HRC, and OFDA delegates participated. It was agreed to establish South East Europe Flash Flood Guidance System (SEEFFGS) making Turkey the regional center.

DHMZ started to prepare and sent data for the establishing SEEFFGS from the year of 2014. The FFGS for Croatia is operational from September 2015. It runs 4 times per day regularly at Regional center in Turkey, Ankara. DHMZ has real time access to the FFGS through its web page (Dashboard console).

Dashboard console has four main toolbars - Inventory Status, Real Time Data Processing Status, Computational Server Status and Dissemination Server Status including Real Time Data Download. The Dashboard is designed primarily for system administrators, but it also has four different products displayed in windows at the top of the console including Global Hydrometeor Estimator (GHE), Meteorological Station Data Reception Status, Average Soil Moisture (ASM) and Forecast Mean Areal Precipitation (FMAP). At the bottom of the dashboard, one can click on a given country and the products displayed in the dashboard will be for that country only. There is a link for the product console at the bottom also, that link move one to the forecaster interface (**Figure 34**).

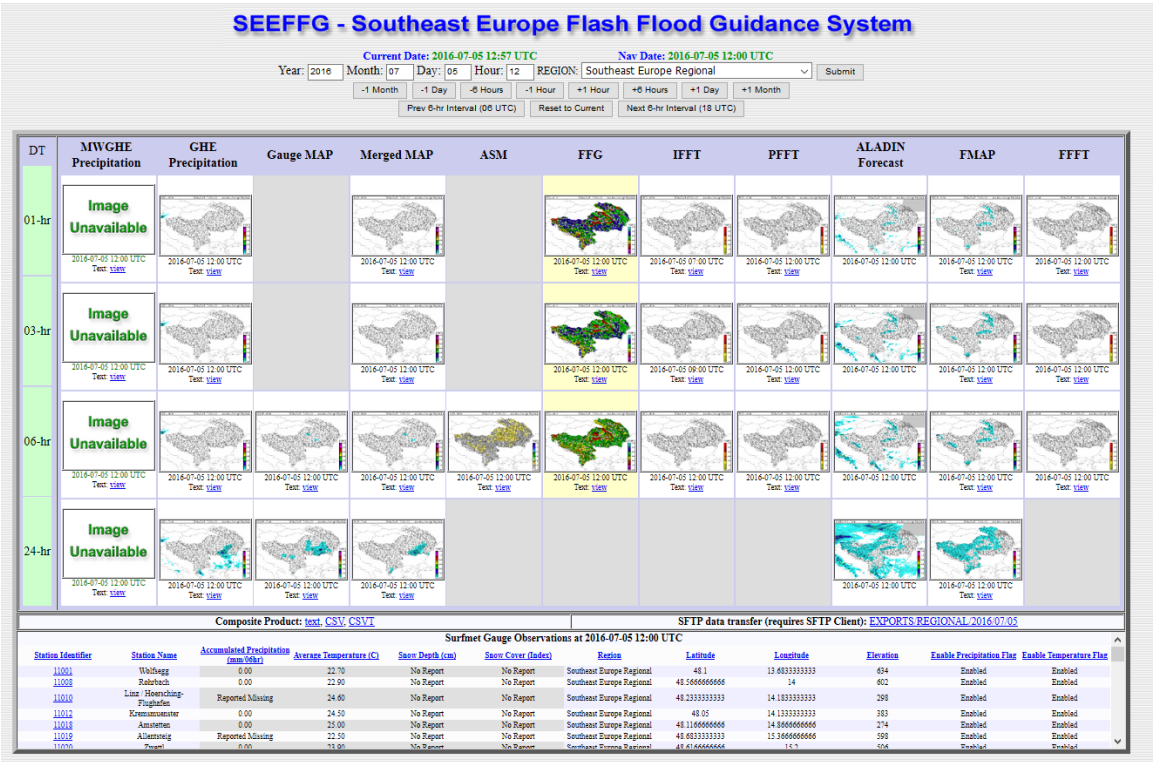

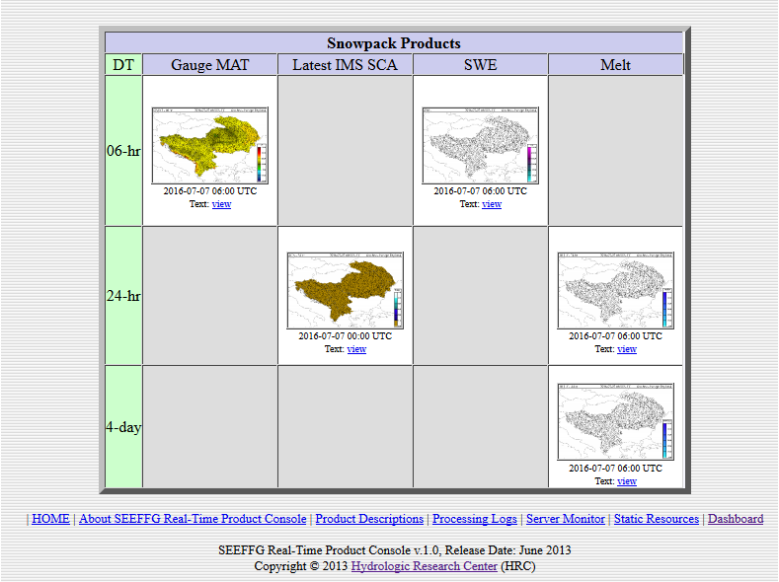

Figure 34 *SEEFFGS Forecasters interface.*

Interface: The products are presented as thumbnails on the interface; clicking on the thumbnail provides a larger image. The main features of the console are as follows:

1. At the top of the main page, products, date and time selection toolbars are provided. A user can use this toolbar to navigate to different dates and times and to display products for selected countries.
2. SEEFFG main products are listed consisting MWGHE (Micro Wave adjusted Global Hydrometeor Estimator) precipitation, GHE (Global Hydrometeor Estimator) satellite precipitation estimates, Gauge MAP (Gauge Mean Areal Precipitation based on gauge data only), Merged MAP (Merged Mean Areal Precipitation), ASM (Average Soil Moisture), FFG (Flash Flood Guidance), IFFT (Imminent Flash Flood Threat), PFFT (Persistence Flash Flood Threat), ALADIN Forecast, FMAP (Forecast Mean Areal Precipitation), FFFT (Forecast Flash Flood Threat).
3. On the left side of the FFGS Products, the time intervals (1, 3, 6, and 24 hour) are displayed.
4. Below the FFGS Products, selected surface meteorological observations (Synoptic Stations) from the member states and disseminated through the WMO GTS (Global Telecommunication System) are displayed.
5. Snow products including Gauged MAT (Mean Areal Temperature), Latest IMS SCA (Snow Coverage Area), SWE (Snow Water Equivalent), and MELT are displayed at the bottom of the main interface.
6. At the bottom of the interface page, products description and system monitoring tools are listed consisting of products description, processing logs, server monitor, static resources and a link back to Dashboard.

The SEEFFG forecaster product console displays product for each sub-basins without any geographical information like cities, roads, border, etc. that could precise determine an event location. DHMZ hydrological forecasters use GIS software before issuing flash flood warnings. For such purposes, Turkish Meteorological Service (regional center) uses GIS sever which will also be available for all member state forecasters.

Verification of flash flood events are not easy task but very important to evaluate the performances of the FFG system. DHMZ collects flash flood event reports (from National Protection and Rescue Directorate and press) for verification purposes.

DHMZ was the leading author of the SEEFFGS User Guide created during 2016. It will be published by WMO and that will be of great help for recent and future forecasters and users of FFGS.

8. References

Bajić, A., Ivatek-Šahdan, S., Žibrat, Z. (2008): ANEMO-ALARM iskustva operativne primjene prognoze smjera i brzine vjetra. GIU Hrvatski cestar. 109-114

Bašták Ďurán, I., J. Geleyn, and F. Váňa, 2014.: doi:10.1175/JAS-D-13- 0203.1

Boloni G. and K. Horvath, 2010: Diagnosis and tuning of background error statistics in a variational data assimilation system**.** *Idojaras*, 114, 1-19.

Branković, Č., I. Güttler, M. Gajić-Čapka (2013): Evaluating climate change at the Croatian Adriatic from observations and regional climate models' simulations. *Clim. Dyn.*, 41, 2353–2373

Catry B., Geleyn J.-F., Tudor M., Bénard P. and Trojakova A. (2007): Flux conservative thermodynamic equations in a mass-weighted framework. Tellus 59A, pp 71–79.

Dee, D.P. and Coauthors (2011): The ERA-Interim reanalysis: configuration and performance of the data assimilation system. *Q. J. R. Meteorol. Soc.*, 137, 553–597

Delle Monache, L., Eckel, T., Rife, D., Nagarajan, B., 2013: Probabilistic weather prediction with an analog ensemble. Monthly Weather Review 141, 3498-3516.

Desroziers G., Berre L., Chapnik B., Poli P., 2005: Diagnosis of observation, background and analysis error statistics in observation space, QJRM, 131, 3385-3396

H. Davies, 1983: Limitations of some common lateral boundary schemesused in regional NWP models, Mon.Wea.Review., 111, 1002-1012

Geleyn J.-F. (1988): Interpolation of wind, temperature and humidity values from model levels to the height of measurement. Tellus, 40A, pp.347–351.

Geleyn J.-F. and Hollingsworth A (1979): An economical analytical method for the computation of the interaction between scattering and line absorption of radiation. Beitr Phys Atmos 52:1–16.

Geleyn J.-F., Benard P. and Fournier, R. (2005a): A general-purpose extension of the Malkmus band-model average equivalent width to the case of the Voigt line profile. Quart. J. Roy. Meteor. Soc. 131:2757–2768

Geleyn J.-F., Fournier R., Hello G., Pristov N. (2005b): A new 'bracketing' technique for a flexible and economical computation of thermal radiative fluxes, scattering effects included, on the basis the Net Exchanged Rate (NER) formalism. WGNE Blue Book

Geleyn J.-F., Vana F., Cedilnik J., Tudor M. and Catry B. (2006): An intermediate solution between diagnostic exchange coefficients and prognostic TKE methods for vertical turbulent transport. WGNE Blue Book

Geleyn J.-F., Catry B., Bouteloup Y. and Brožkova, R. (2008): A statistical approach for sedimentation inside a microphysical precipitation scheme. Tellus 60A,649–662

Gerard, L. (2007): An integrated package for subgrid convection, clouds and precipitation compatible with the meso gamma scales. Quart. J. Roy. Meteor. Soc., 133, 711–730.

Gerard, L. and Geleyn, J.-F. (2005): Evolution of a subgrid deep convection parameterization in a limited area model with increasing resolution. Quart. J. Roy. Meteor. Soc., 131, 2293–2312.

Gerard, L., Piriou, J.-M., Brožková, R., Geleyn, J.-F. and Banciu, D. (2009): Cloud and Precipitation Parameterization in a Meso-Gamma-Scale Operational Weather Prediction Model. Mon. Wea. Rev., 137, 3960–3977.

Giard, D. and Bazile, E. (2000): Implementation of a new assimilation scheme for soil and surface variables in a global NWP model. Mon. Wea. Rev. 128, 997-1015.

Giorgi, F., E. Coppola, F. Solmon, L. Mariotti, M.B. Sylla, X. Bi, N. Elguindi, G.T. Diro, V. Nair, G. Giuliani, S. Cozzini, I. Güttler, T.A. O'Brien, A.B. Tawfik, A. Shalaby, A.S. Zakey, A.L. Steiner, F. Stordal, L.C. Sloan, C. Brankovic (2012): RegCM4: Model description and preliminary tests over multiple CORDEX domains. *Clim. Res.*, 52, 7–29

Güttler, I., Č. Branković, L. Srnec, M. Patarčić (2014): The impact of boundary forcing on RegCM4.2 surface energy budget. *Climatic Change*, 125, 67–78

Haiden, T., A. Kann, C. Wittmann, G. Pistotnik, B. Bica, Gruber, C. (2011): The Integrated Nowcasting through Comprehensive Analysis (INCA) System and Its Validation over the Eastern Alpine Region. Wea.Forecasting, 26, 166 183.

Haylock, M.R., N. Hofstra, A.M.G. Klein Tank, E.J. Klok, P.D. Jones and M. New (2008): A European daily high-resolution gridded dataset of surface temperature and precipitation. *J. Geophys. Res (Atmospheres)*, 113, D20119, doi:10.1029/2008JD10201

Hazeleger, W. and Coauthors (2010). EC-Earth: A seamless Earth-system prediction approach in action *Bull. Amer. Meteor. Soc.*, 91, 1357-1363

Horvath, K., D. Koracin, R. K. Vellore, J. Jiang, and R. Belu, 2012: Sub-kilometer dynamical downscaling of near surface winds in complex terrain using WRF and MM5 mesoscale models. J. Geophys. Res., 117, D11111, 19pp., doi:10.1029/2012JD017432.

Horvath, K., Bajić, A., & Ivatek-Šahdan, S. (2011): Dynamical Downscaling of Wind Speed in Complex Terrain Prone To Bora-Type Flows. J. Appl. Meteor. Climatol., 50, 1676–1691.

Horvath, K., Ivatek-Šahdan, S., Ivančan-Picek, B. and Grubišić, V. (2009): Evolution and structure of two severe cyclonic bora events: contrast between the northern and southern Adriatic. Weather and forecasting 24, 946-964.

Iršić, M., Predoš, A., Zgonc, T., Strelec Mahović, N. (2004): CEI Nowcasting tools based on remote sensing data in Croatia and Slovenia. Proceedings - 2004 EUMETSAT Meteorological Satellite Conference, Prague, Czech Republic, 31 May - 04 June 2004.

Ivatek-Šahdan, S. & Ivančan-Picek, B. (2006): Effects of different initial and boundary conditions in ALADIN/HR simulations during MAP IOPs. Meteorol. Z. 15, 187–197.

Ivatek-Šahdan, S. & Tudor M. (2004): Use of high-resolution dynamical adaptation in operational suite and research impact studies. Meteorol Z 13(2):1–10

Janeković, I. Mihanović, H. Vilibić, I. Tudor, M. (2014) Extreme cooling and dense water formation estimates in open and coastal regions of the Adriatic Sea during the winter of 2012. Journal of geophysical research : oceans. 119 , 5; 3200-3218.

Jeričević, A., Kraljević, L., Vidič, S., and Tarrasón, L. (2007): Project description: High resolution environmental modelling and evaluation programme for Croatia (EMEP4HR), Geofizika, 24 (2), 137-143, available form http://geofizika-journal.gfz.hr/vol24.htm.

Jeričević, Amela; Večenaj, Željko (2009): Improvement of vertical diffusion analytic schemes under stable atmospheric conditions. Boundary - Layer Meteorology. 131, 2; 293-307.

Jeričević, Amela; Kraljević, Lukša; Grisogono, Branko; Fagerli, Hilde; Večenaj, Željko (2012): Parameterization of vertical diffusion and the atmospheric boundary layer height determination in the EMEP model. Atmospheric chemistry and physics. 10, 2; 341-364.

Jeričević, Amela; Fagerli, Hilde; Grisogono, Branko (2011): Exploring the properties of local and non-local vertical diffusion schemes in the EMEP model using 222Rn data. International journal of environment and pollution. (in press)

Kalinić, H. Mihanović, H. Cosoli, S. Tudor, M. Vilibić, I. (2016) Predicting ocean surface currents using numerical weather prediction model and Kohonen neural network: a northern Adriatic study. // Neural Computing and Applications. 11(in press)

Kessler, E., 1969. On distribution and continuity of water substance in atmospheric circulations. Meteorol Monogr Am Meteorol Soc 10(32):84.

Kraljević, L., Belušić, D., Bencetić Klaić, Z., Bennedictow, A., Fagerli, H., Grisogono, B., Jeričević, A., Mihajlović, D., Špoler Čanić, K., Tarrasón, L., Valiyaveetil, S., Vešligaj, D., and Vidič, S. (2008): Application of EMEP Unified model on regional scale – EMEP4HR, Croat. Meteorol. J., 43, Proceedings from a 12 HARMO conference Part 1: Oral Presentations, /Đuričić, Vesna (Ed.), Zagreb, 151-151, available from http://www.harmo.org/Conferences/Proceedings/Cavtat/topicIndex.asp?topicID=0.

Lu, C., Yuan, H., Schwartz, B. E., Benjamin, S.G:, 2007: Short-Range Numerical Weather Prediction Using Time Lagged Ensembles. Weather and Forecasting, 22, 580-595.

Mikuš, P., Bedka, K., Strelec Mahović, N. (2011): Comparison and validation of satellite-based overshooting top detection methods. Proceedings - 6th European Conference on Severe Storms (ECSS 2011), Palma de Mallorca, Spain, 03-07 October 2011.

Mikuš, P., Strelec Mahović, N. (2011): Correlating overshooting tops and severe weather. Proceedings - 6th European Conference on Severe Storms (ECSS 2011), Palma de Mallorca, Spain, 03-07 October 2011.

MZOIP (2014) Sixth National Communication and First Biennial Report of the Republic of Croatia under the United Nation Framework Convention on the Climate Change. Republic of Croatia Ministry of Environmental and Nature Protection (MZOIP), Zagreb, pp 247

Odak Plenković, I., Delle Monache, L., Horvath, K., Hrastinski, M. (2018): Deterministic Wind Speed Predictions with Analog-based Methods over Complex Topography. Journal of Applied Meteorology and Climatology (accepted).

Patarčić, M. and Branković, Č. (2012): Skill of 2-m temperature seasonal forecasts over Europe in ECMWF and RegCM models. Monthly Weather Review 140, 1326-1346.

Patarčić, M., M. Gajić-Čapka, K. Cindrić, Č. Branković (2014) Recent and near-future changes in precipitation-extreme indices over the Croatian Adriatic coast. *Climate Research*, 61:157-176

Solazzo, E.; Roberto, Bianconi; Robert, Vautard; K. Wyat, Appel; Bertrand, Bessagnet; Jørgen, Brandt; Jesper H., Christensen; Charles, Chemel; Isabelle, Coll15, Hugo, Denier van der Gon; Joana, Ferreira; Renate, Forkel; Xavier, V. Francis; George, Grell; Paola, Grossi; Ayoe B., Hansen; Jeričević, Amela; Lukša, Kraljević; Ana Isabel, Miranda; Michael D., Moran; Uarporn, Nopmongco; Guido, Pirovano; Marje, Prank; Angelo, Riccio; Karine N., Sartelet; Martijn, Schaap; Jeremy D., Silver; Ranjeet S., Sokhi; Julius, Vira; Johannes, Werhahn; Ralf, Wolke; Greg, Yarwood; Junhua, Zhang; S.Trivikrama, Rao; StefanoGalmarini (2011): Model evaluation and ensemble modelling of surface level ozone in Europe and North America in the context of AQMEII. Atmospheric environment (1994). (in print)

Srnec, L., K. Cindrić, I. Güttler, Č. Branković (2014) Simulation of extremely hot events in Croatia with RegCM4, 20th International Congress of Biometeorology, Cleveland, OHIO, USA, 28.09.-2.10.2014.

Stanešić, A. (2011). Assimilation system at DHMZ: Development and first verification results. Cro. Met. J. 44/45, 3-17.
Strelec Mahović, N. (2005): Operational use of Meteosat-8 SEVIRI data and derived nowcasting products. Proceedings - 2005 EUMETSAT Meteorological Satellite Conference, Dubrovnik, Croatia, 19-23 September 2005.
Strelec Mahović, N. and Zeiner, B. (2009): Application of Meteosat SEVIRI channel difference 0.6 μm - 1.6 μm in convective cells detection. Atmos. res. 93, 1-3, 270-276
Strelec Mahović, N., Mikuš, P. (2011): Correlating locations of the overshooting tops with the occurrence of severe weather on the ground. Proceedings - 2011 EUMETSAT Meteorological Satellite Conference, Oslo, Norway, 05-09 September 2011.
Telišman Prtenjak, Maja; Jeričević, Amela; Kraljević, Lukša; Herceg Bulić, Ivana; Nitis, Theodoros; Bencetić Klaić, Zvjezdana (2009): Exploring atmospheric boundary layer characteristics in a severe SO2 episode in the north-eastern Adriatic. Atmospheric chemistry and physics. 9, 13; 4467-4483.
Tudor M. (2010): Impact of horizontal diffusion, radiation and cloudiness parameterization schemes on fog forecasting in valleys. Met. Atm. Phy. Vol.108, pp. 57-70.
Tudor, M. (2011): The meteorological aspects of the DART field experiment and preliminary results. Cro. Met. J. 44/45, 31-46.
Tudor, M. and Ivatek-Šahdan, S. (2002): The MAP-IOP 15 case study. Cro. Met. J. 37, 1-14.
Tudor, M. and Ivatek-Šahdan, S. (2010): The case study of bura of 1st and 3rd February 2007, Meteorol. Z., 19, pp. 453-466.
Tudor, M., Termonia, P., (2010): Alternative formulations for incorporating lateral boundary data into limited-area models. Mon. Wea. Rev. 138, pp. 2867-2882.
Tudor, M., 2013. A test of numerical instability and stiffness in the parametrizations of the ARPÉGE and ALADIN models. Geoscientific model development, 6, 901-913.
Tudor, M., 2015. Methods for automatized detection of rapid changes in lateral boundary condition fields for NWP limited area models. Geoscientific Model Development. 8, 2627-2643.
Tudor, M. Stanešić, A. Ivatek-Šahdan, S. Hrastinski, M. Odak Plenković, I. Horvath, K. Bajić, A. Kovačić, T.(2015a) Changes in the ALADIN operational suite in Croatia in the period 2011-2015. Cro. Meteorol. Jour. 50, 71-89.
Tudor, M. Stanešić, A. Ivatek-Šahdan, S. Hrastinski, M. Odak Plenković, I. Horvath, K. Bajić, A. Kovačić, T.(2015b) Operational validation and verification of ALADIN forecast in Meteorological and Hydrological Service of Croatia. Cro. Meteorol. Jour 50, 47-70.
Váňa F., Bénard P., Geleyn J.-F., Simon A. & Seity Y. (2008): Semi-Lagrangian advection scheme with controlled damping–an alternative way to nonlinear horizontal diffusion in a numerical weather prediction model. Quart. J. Roy. Meteor. Soc, Vol.134, pp. 523–537.
Van der Linden P, Mitchell JFB (eds) (2009) ENSEMBLES: climate change and its impacts: summary of research and results from the ENSEMBLES project. Met Office Hadley Centre, FitzRoy Road, Exeter EX1 3 PB, UK, p 160
Vautard, Robert; Moran, Michael D.; Solazzo, Efisio; Gilliam, Robert C.; Matthias, Volker; Bianconi, Roberto; Chemel, Charles; Ferreira, Joana; Geyer, Beate; Hansen, Ayoe B.; Jeričević, Amela; Prank, Marje; Segers, Arjo; Silver, Jeremy D.; Werhahn, Johannes; Wolke, Ralf; Rao, S.T.; Galmarini, Stefano (2011).
Evaluation of the meteorological forcing used for the Air Quality Model Evaluation International Initiative (AQMEII) air quality simulations. Atmospheric environment (1994). (in press).
Vilibić, I. Šepić, J. Mihanović, H. Kalinić, H. Cosoli, S. Janeković, I. Žagar, N. Jesenko, B. Tudor, M. Dadić, V.

Ivanković, D. (2016a) Self-Organizing Maps-based ocean currents forecasting system. Scientific Reports. 6 ()

Vilibić, I. Kalinić, H. Mihanović, H. Cosoli, S. Tudor, M. Žagar, N. Jesenko, B. (2016b) Sensitivity of HF radar-derived surface current self-organizing maps to various processing procedures and mesoscale wind forcing. Computational geosciences. 20, 115-131.

Wang, Y., Bellus, M., Wittmann, C., Steinheimer, M., Weidle, F., Kann, A., Ivatek-Šahdan, S., Tian, W., Ma, X., Tascu, S., Bazile, E. (2011): The Central European limited-area ensemble forecasting system: ALADIN-LAEF. Quart. J. Roy. Meteor. Soc 137, 483-502.

Vautard, R., A. Gobiet, D. Jacob, M. Belda, A. Colette, M. Déqué, J. Fernández, M. Garica-Díez, K. Goergen, I. Güttler, T. Halenka, T. Karakostas, E. Katragkou, K. Keuler, S. Kotlarski, S. Mayer, G. Nikulin, M. Patarčić, J. Scinocca, S. Sobolowski, M. Suklitsch, C. Teichmann, E. van Meijgaard, K. Warrach-Sagi, V. Wulfmeyer, P. Yiou (2013): The simulation of European heat waves from an ensemble of regional climate models within the EURO-CORDEX project. *Clim. Dyn*., 41, 2555–2575

Wilks, D. S. (2006.): Statistical methods in the atmospheric sciences. Second Edition. Academic Press, London.

Žagar, M. and J. Rakovec, (1999): Small-scale surface wind prediction using dynamic adaptation. Tellus 51, 489-504.